PHYSICAL REVIEW B VOLUME 39, NUMBER 10 1 APRIL 1989

Charging effects and quantum properties of small superconducting tunnel junctions

M. Iansiti, M. Tinkham, A. T. Johnson, Walter F. Smith, and C. J. Lobb
Department of Physics and Division of Applied Sciences, Harvard University, Cambridge, Massachusetts 02138
(Received 2 August 1988; revised manuscript received 23 November 1988)

We have fabricated small superconducting tunnel junctions with a large single-electron charging energy E_c and measured the low-temperature current-voltage characteristics of devices having a wide range of ratios of E_c to the Josephson coupling energy E_J. For $E_c \approx E_J$, the I-V curve is resistive at all currents and the critical current is greatly reduced relative to that of conventional Josephson junctions. If $E_J \ll E_c$, we find a novel regime in which aspects of the Coulomb blockade of tunneling *coexist* with features typical of Josephson tunneling. We describe a number of models which appear to explain the salient new features of our observations. In the high-temperature regime, thermal activation and damping effects are very important, since E_c and E_J are only of order 1 K, and the experimental results are fitted by extending well-established classical methods. At low temperatures, however, quantum fluctuations of the phase appear to become much more important, as thermal fluctuations and quasiparticle damping freeze out. We thus present a number of quantum-mechanical treatments, based in phase and charge space, which provide a semiquantitative account of the measurements in the low-temperature regime.

I. INTRODUCTION

In this paper we investigate the dynamics of mesoscopic superconducting tunnel junctions. Our study is based on measurements of the current-voltage (I-V) characteristics of high-resistance low-capacitance Josephson junctions, whose single-electron charging energy $e^2/2C$ is comparable to, or greater than, the other relevant energies.[1-3]

The dynamics of a Josephson device may be described by a Hamiltonian H, which is a function of the phase difference ϕ between the wave functions of the two electrodes, and the charge Q transferred between the electrodes. Ignoring dissipation, we write

$$H(\phi,Q)=E_c(Q/e)^2-E_J\cos\phi \ . \tag{1}$$

The effect of a current bias can be incorporated by adding a term equal to $-(\hbar/2e)I\phi$, where I is the bias current. The character of the dynamics describing a Josephson device thus depends fundamentally on the ratio of two energies: E_J, the Josephson coupling energy [$E_J=(h/8e^2)(\Delta/R_n)$, for an ideal tunnel junction at low temperatures], and E_c, the charging energy ($E_c=e^2/2C$). Δ is the superconducting energy gap, R_n is the normal resistance, and C is the capacitance of the device. For conventional junctions, the dominant energy in the problem is the Josephson coupling energy and the most important term in $H(\phi,Q)$ is the one associated with E_J. The state of the system at low currents is then simply obtained by the minimization of energy by a classically well-defined ϕ value at the minimum of a well of the tilted cosinusoidal potential. The phase ϕ is thus "trapped" in a potential well until the tilt imposed on the Josephson potential by the current bias is enough to allow it to escape. This results in the I-V characteristic features shown in Fig. 1(a); a *zero* resistance branch at low currents, and a very sharp jump to the dissipative voltage state at a critical current I_c.

In recent years, by fabricating very small tunnel junctions,[4] granular films,[5-8] or by using a scanning tunneling microscope[9,10] (STM), it has been possible to study devices in which the charging energy dominates over the other energies of the system (such as k_BT or E_J). This has been achieved in samples with both normal and superconducting electrodes. In normal samples, a typical low-temperature I-V response is shown in Fig. 1(b). The transfer of an electron from one electrode to the other involves an energy change of $e^2/2C$. At low voltages *charge* is thus trapped, and the resistance is very high, until the system acquires enough energy from the biasing source to enable an electron to tunnel to the other electrode. At this point ($V\approx e/2C$) the dynamic resistance decreases, producing a knee in the I-V curve. This effect is known as the "Coulomb blockade."[11]

A similar effect is observed in superconducting samples[4] in which the charging energy is much larger than the Josephson coupling energy. As a result the knee at $V=e/2C$ is superimposed on the superconducting energy gap, as shown schematically in Fig. 1(c). In a broad sense, this effect is *conjugate* to the Josephson effect described above. In conventional devices ϕ is a "well-defined" semiclassical variable. When the charging energy is dominant and the Josephson coupling energy is insignificant, quantum fluctuations in ϕ are very large and the quantum-mechanical conjugate Q (the charge difference between the electrodes) may now be treated classically. The resulting dynamics are very different: the zero-resistance branch up to $I=I_c$ of the Josephson effect I-V curve is replaced by a very high-resistance branch with no critical current.

Our study explores the crossover region *between* the two extremes described above. By varying the ratio $x\equiv E_c/E_J$, we sweep from a regime in which the Joseph-

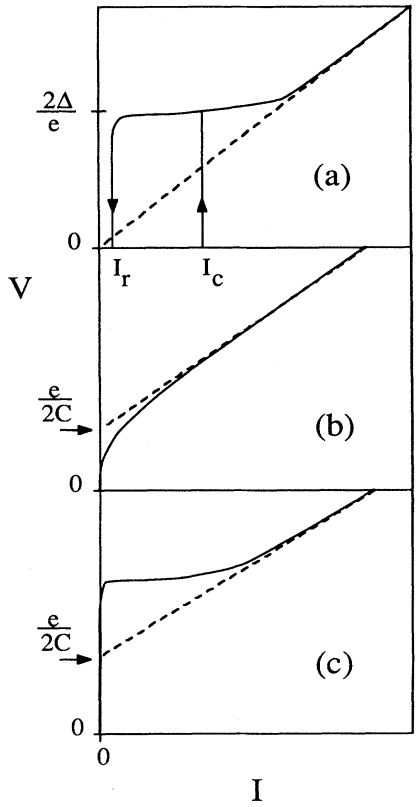

FIG. 1. Schematics of typical tunnel junction *I-V* characteristics. (a) Underdamped superconductor-insulator-superconductor tunnel junction with $E_J \gg E_c, k_B T$. (b) Normal-insulator-normal tunnel junction with $E_c \gg k_B T$. (c) Superconductor-insulator-superconductor tunnel junction with $E_c \gg E_J, k_B T$.

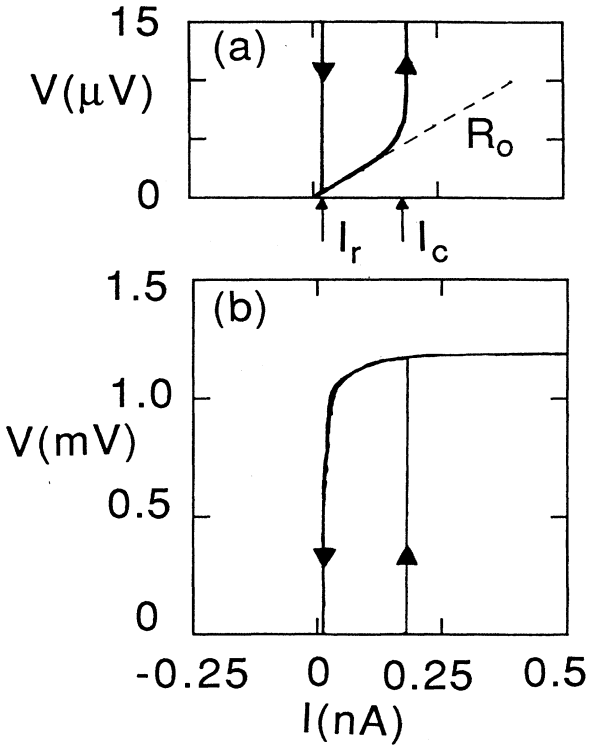

FIG. 2. *I-V* curve of a sample with $R_n = 70$ kΩ and estimated capacitance $C \approx 1$ fF, taken at $T = 0.98$ K and $H = 0$, showing definitions of I_c, I_r, and R_0. Parts (a) and (b) have the same horizontal scale but different vertical scales.

son coupling energy is large, well into the regime in which the charging energy appears to dominate. Experimentally, we have achieved this in two different ways. First, we have constructed samples of different areas and oxide barrier thicknesses, which have allowed us to go from $x \approx \frac{1}{100}$ to $x \approx 10$. Second, we have further decreased E_J by applying a magnetic field, which has enabled us to study the system with x values in principle approaching infinity, as $E_J \to 0$.

If the Josephson energy is much larger than $e^2/2C$, we obtain results typical of conventional Josephson devices [as sketched in Fig. 1(a)]. As the Josephson and charging energy become of comparable magnitude, however, we observe two novel regimes.[1-3,12] First, we find that as E_J becomes of order E_c, the critical current is greatly reduced and the *I-V* curve becomes resistive, even at very low bias currents, as shown in Fig. 2. Second, if the Josephson coupling is reduced further by applying a magnetic field, we observe the new type of *I-V* curve shown in Fig. 3. The striking feature is the *coexistence* of a plateau beginning at $V_b \cong e/2C$, reminiscent of Coulomb blockade measurements made on samples in which E_c is completely dominant, with other features common to Josephson tunneling, such as a sharp jump from the plateau voltage of the superconducting energy gap voltage at a "critical current" I_c. If the Josephson coupling is reduced even further, we recover Coulomb blockade results: The critical current goes to zero, and if the field is large enough to destroy the superconductivity, an *I-V*

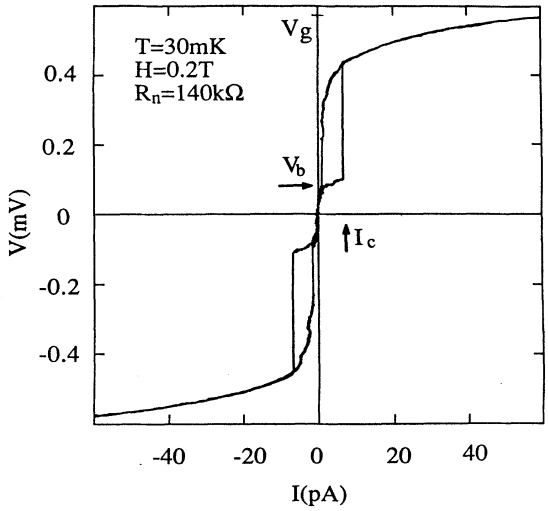

FIG. 3. *I-V* characteristic of a single Josephson junction $R_n = 140$ kΩ and estimated $C \approx 1$ fF in a magnetic field of 0.2 T at $T = 30$ mK.

curve analogous to that shown in Fig. 1(b) is observed.

In this paper, we discuss these observations, and explore their interpretation in some detail. We begin by providing an account of our experiments in Sec. II. We cover the methods used in the fabrication and measurement of the samples in Sec. II A. Next, in Sec. II B, we summarize our experimental results. Section III contains a discussion of models used in interpreting our results. We first define the basic models used in Sec. III A. Second, in Sec. III B, we examine the semiclassical models used in interpreting earlier work to see to what extent they can explain the new data by simply taking account of the new parameter regimes involved. This treatment is partially successful in interpreting our higher-temperature results, as thermal fluctuations apparently overwhelm quantum-mechanical fluctuations. Third, in Secs. III C and III D, we investigate to what extent the introduction of a more fully quantum-mechanical picture, including large quantum uncertainties in the phase, can account for the remaining features. Section III C approaches the problem in ϕ space, which is a natural extension of our semiclassical treatment of Sec. III B. Section III D approaches the problem in Q space, which is more appropriate in the large charging energy limit. We conclude in Sec. IV.

II. THE EXPERIMENT

A. Experimental techniques

The junctions are patterned[13,14] using electron-beam lithography. We begin by coating an oxidized silicon substrate with a thick layer of PMMA/MAA (polymethylmethacrylate/methacrylic acid) polymer resist (spun at 3000 rpm) and a thin layer of PMMA (spun at 8000 rpm). Next, the substrate stencils are exposed using a modified JEOL 31U scanning electron microscope and developed in methylisobutylketone (MIBK). We have found that the optimal combination of large undercut (>1 μm) and small linewidth (~ 0.2 μm) may be obtained by the combination of very low beam current (~ 4 pA), low beam voltage (10–12 kV), short exposure time, and long development time (5–15 min). The structures resulting from this process are of the suspended bridge type commonly used for resist-aligned junction fabrication. The device is then fabricated by thermally evaporating the first tin electrode, oxidizing by a dc glow discharge, and thermally evaporating the second tin electrode. Following the resist-aligned method, the evaporations are performed at different angles with respect to the substrate normal to insure junction overlap under the resist bridge. The junction leads are made of tin in the immediate vicinity of the junction (~ 20 μm). Their thickness is about 800 Å. The remaining leads, patterned by photolithography, are made of 400 Å of Au evaporated on top of 50 Å of Cr. A scanning electron microscope photograph of one of our junctions is shown in Fig. 4.

The junctions were measured in a top-loading Oxford Instruments dilution refrigerator. To avoid shorts through the oxide barrier, possibly caused by tin whisker growth, the samples were cooled within a few hours of the evaporation. Once below liquid-helium temperature, however, the junctions could be measured without observing any significant degradation for several weeks.

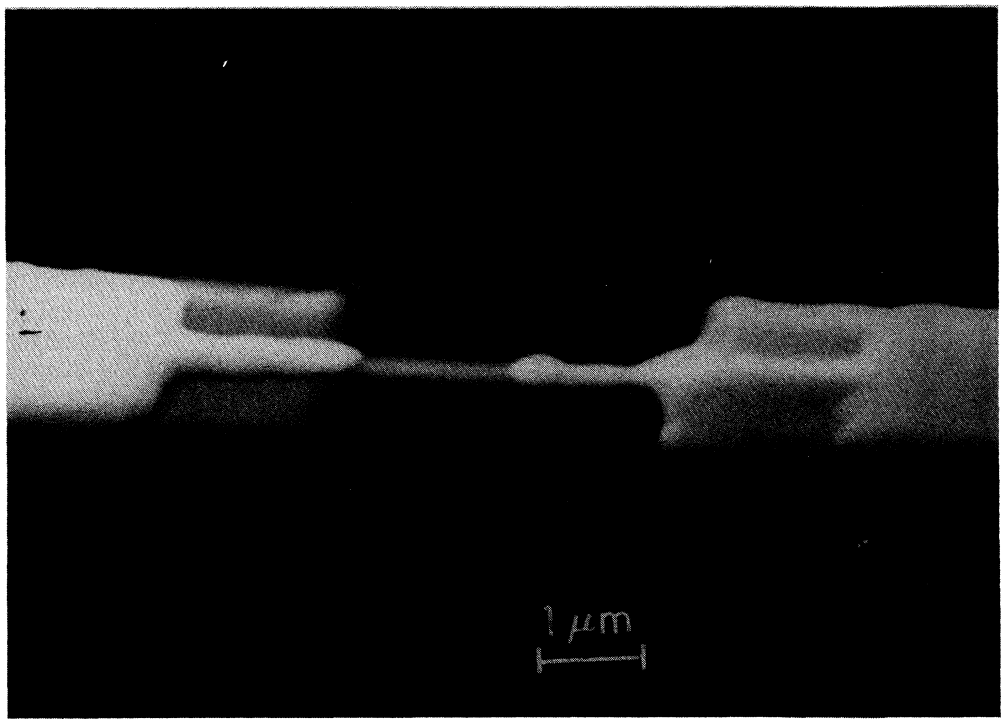

FIG. 4. Scanning electron microscope photograph of a previously measured sample with area 0.1 $(\mu m)^2$, normal resistance $R_n = 35$ kΩ, and capacitance $C \approx 2$ fF.

TABLE I. Sample parameters: R_n is the normal resistance of the junction. R_{L0} is the low-temperature leakage resistance. $T_{\min}$ is the lowest temperature at which measurements were carried out. Area is the area of the sample, from scanning electron microscope photographs. C is the capacitance of the sample; C was estimated by Coulomb blockade measurements in samples 4, 5, 8, and 11; for the other samples, the estimate C was given by the geometrical capacitance. E_J is the $T=0$ Josephson energy and E_c is the single electron charging energy, defined in the text. N_{JJ} is the total number of junctions present in a sample; the junctions were patterned in a linear array and the quoted measurements correspond to the lowest I_c (highest resistance) junction in the array.

Sample	R_n (kΩ)	R_{L0} (kΩ)	$T_{\min}$ (K)	Area [$(\mu m)^2$]	C (fF)	E_J (K)	E_c (K)	N_{JJ}
1	0.52	10	1.4	0.1	2	40	0.45	2
2	3.4	105	1.8	0.15	3	6.2	0.3	1
3	6.5	3 000	0.85	0.4	7	3.2	0.15	2
4	8.5	4 000	0.02	0.15	3.5	2.7	0.3	1
5	14.8	2 860	0.02	0.1	2.5	1.4	0.35	1
6	30	2 500	1.3	0.025	<1	0.7	>0.9	2
7	~ 30		0.02	0.1	2	0.7	0.45	11
8	34	2 400	0.02	0.1	2	0.6	0.45	1
9	70	40 000	0.02	0.04	1	0.3	0.9	2
10	110		0.02	0.05	1	0.19	0.9	2
11	140	300 000	0.02	0.05	1	0.15	0.9	1

The samples were isolated from the environment by *RLC* filtering composed of 10-kΩ cold resistors and the extensive distributed inductance and capacitance of the leads. The measured cutoff frequency of the leads was below 1 kHz. The dilution refrigerator was enclosed in an electrically screened room, to avoid rf pickup. In addition, to minimize the extrinsic noise fed into the sample by the measurement setup, the latter was kept very simple: The current source was composed of a dry battery, whose voltage was adjusted by a variable voltage divider, and a 500-MΩ current-limiting resistor. The voltage was measured by a PAR 113 preamp and a Hewlett Packard analog *XY* recorder. The power levels required to measure R_0 and I_c (defined in the next section) were in general quite small, in the low-femtowatt range.

An important part of our analysis is the estimation of the *intrinsic* capacitance of the junction, defined in this context as the capacitance due *only* to the parallel plate geometry of the superconducting electrodes separated by the oxide barrier through which the tunneling occurs. The intrinsic capacitance is given by $C_i=\epsilon_0\epsilon_r A/d$. A is the junction area, obtained from scanning electron microscope photographs. We use a dielectric constant $\epsilon_r \approx 6$ typical[15,16] of Sn oxide barriers grown by glow discharge, and a barrier thickness $d \approx 25 \pm 5$ Å, which is quite reasonable for our junctions, given their very low current density (and thick barriers). Table I contains a list of sample parameters.

B. Experimental results

Our observations can be classified into two regimes.

1. *Regime of comparable charging and Josephson energy*

A typical *I-V* curve for a high-resistance, low-capacitance junction in the first regime is shown in Fig. 2. Figure 2(a) has the same horizontal scale as 2(b), but a hundred times more sensitive vertical scale. The estimated value of $x=E_c/E_J$ for this sample is 2.4. Similar *I-V* curves were also observed by Ono *et al.*[17]

The *I-V* curve displays *two* different measurable critical currents, I_c and I_r. I_c is the maximum current that can be carried before the jump into the high-voltage regime. I_r, the recapture critical current, is the current at which the system returns to the low-voltage state. The familiar "zero-voltage state" is *not* found in this type of junction at *any* current level, as is evident from looking at Fig. 2(a). The behavior of the system is always observably dissipative, and can be characterized by the resistances described below. Our definitions of critical currents are thus modified from the standard ones and are motivated by the need to describe our observations. Our interpretation of these critical currents is developed in the remainder of this paper.

In a classic device, neglecting fluctuations, I_c is given by the value I_{c0} related to E_J by $E_J=\hbar I_{c0}/2e$, where I_{c0} monotonically increases with decreasing temperature.[18] In Fig. 5(a) we display the temperature dependence of I_c and I_r for the junction with 70 kΩ normal resistance. Note the remarkable temperature dependence of I_c, first rising, then dropping by a factor of 10, then rising again by a similar factor as T is reduced. This is very different from the monotonic rise of $I_{c0}(T)$. Moreover, the measured value ($I_c=1.2$ nA) at low temperatures is much less than the theoretical $I_{c0}(T=0)=14$ nA. Another important observation is that the plotted I_c values are averages over a very *narrow* distribution of switching currents measured on repeated sweeps, with width ΔI_c of only $\sim 0.05 I_c \approx 0.003 I_{c0}$. Finally, note that $I_c=I_r$ for $T/T_c > 0.6$, where the *I-V* curve is not hysteretic.

In Fig. 6, we display the temperature dependence of I_c for a number of different samples. The striking nonmonotonic behavior sets in as the sample resistance becomes of the order of ~ 10 kΩ. Our lowest resistance junctions exhibit a monotonic temperature dependence. Moreover, the measured critical current depression is not as marked as in the high resistance samples, and can be accounted for quite well by conventional premature

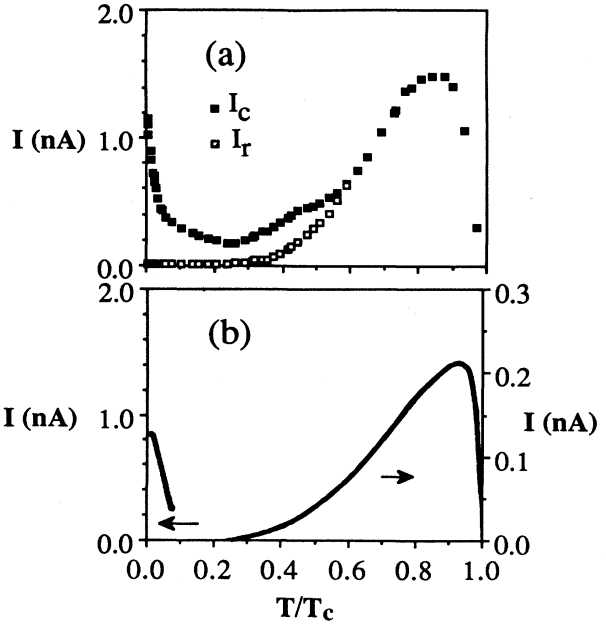

FIG. 5. (a) I_c and I_r vs T for the sample with $R_n = 70$ kΩ. (b) Left: predicted low-temperature I_c, due to Zener tunneling and thermal activation. Right: predicted $I_r(T)$, described in the text.

switching arguments.

As mentioned above, the behavior of our device always appears dissipative; to describe it, we discuss *three* directly measurable resistance values. Using the sample in Fig. 2 as an example, we have the normal-state resistance $R_n \approx 70$ kΩ, the low-voltage resistance R_0 (which ranges from 70 kΩ near the transition temperature T_c down to ~ 1 kΩ as $T \to 0$), and the subgap leakage resistance R_L (ranging from 70 kΩ at T_c up to 40 MΩ as $T \to 0$). The latter is defined by the slope of the quasilinear part of the decrease in V from the gap voltage, measured on an expanded current scale.

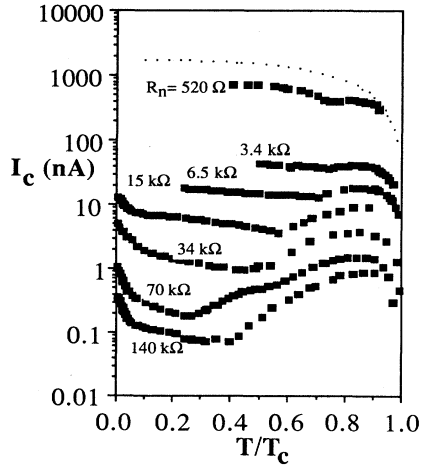

FIG. 6. I_c vs T for seven different samples. The normal resistance of each sample is shown. The solid curve is $I_{c0}(T)$ for the sample with $R_n = 550$ Ω.

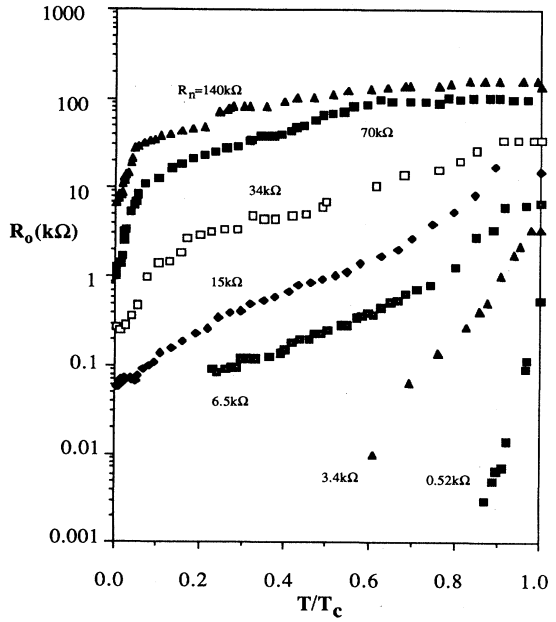

FIG. 7. R_0 vs T for seven samples. For T below $\sim 0.85T_c$ for the sample with $R_n = 520$ Ω, and below $0.60T_c$ for the sample with $R_n = 3.4$ kΩ, R_0 was below our experimental resolution.

In Fig. 7, we display the temperature dependence of $R_0(T)$, for a number of different samples. While for low resistance samples R_0 soon becomes immeasurably small below T_c, resembling the behavior of conventional devices, as R_n becomes of the order of 10 kΩ the behavior changes, and R_0 is significant over the whole temperature range. Concentrating on the 140-kΩ sample, for example, as T is reduced below T_c, where $R_0 = R_n$, R_0 drops, slowly at first, and then more sharply below $0.1T_c$.

Figure 8 shows a plot of the measured R_L versus T for a typical sample. For our samples, the leakage resistance is found to be well approximated by a shunt combination of a thermally excited quasiparticle term $\sim R_n e^{\Delta/k_B T}$ and a residual conductance at $T = 0$:

$$R_L^{-1}(T) \approx R_L^{-1}(0) + R_n^{-1} e^{-\Delta/k_B T} . \quad (2)$$

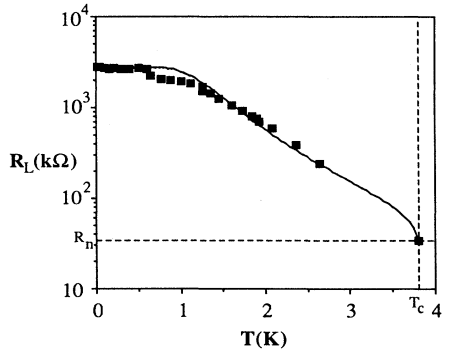

FIG. 8. R_L vs T for the sample with $R_n = 34$ kΩ. The solid line is the fit using Eq. (2).

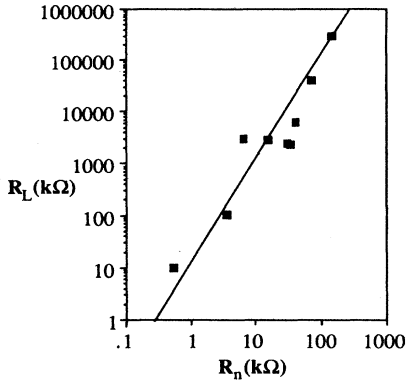

FIG. 9. Low-temperature leakage resistance vs the normal resistance for all measured junctions. The solid line has slope 2 and indicates the trend of proportionality between $R_L(0)$ and R_n^2.

In all measured samples, the oxide barriers were found to be of very high quality, with $R_L(0) \approx 100-10\,000 R_n$. The measured low-temperature leakage resistance $R_L(0)$ is plotted in Fig. 9 as a function of R_n. The trend is for $R_L(0)$ to be roughly proportional to R_n^2, as discussed further in Sec. III A.

Summarizing, the novel phenomena to be understood in this regime are (1) the existence and magnitude of $R_0(T)$; (2) the reentrant temperature dependence of I_c and I_r; and (3) the reduction of I_c by an order of magnitude relative to I_{c0}, while maintaining a narrow switching distribution.

2. *Regime of very small Josephson energy*

To further investigate the crossover from the small-x to the large-x regime, we have found it very convenient to use a parallel magnetic field to control the Josephson coupling energy E_J. The field reduces the Josephson coupling between the electrodes by phase modulation and by reducing the energy gap, both leading to a smaller effective E_J. A typical low-temperature I_c-versus-H curve is shown in Fig. 10. In almost all our junctions, the magnetic field monotonically reduced I_c. This absence of the ideal $\sin x/x$ dependence may be ascribed to the nonuniformity of the device. Since part of the junction area is on the edge of the electrode and part on top, the field orientation is different in different parts of the device. Moreover, in a junction of this sort, fabricated using very long oxidation times, we expect the distribution of the current through the barrier to be nonuniform. The monotonic depression of the energy gap caused by the large magnetic fields used also contributes to the nonideal I_c-versus-H dependence.

Figure 11 shows a sequence of I-V curves taken on the sample with 140 kΩ normal resistance. While at low fields the observed I-V curves are only moderately resis-

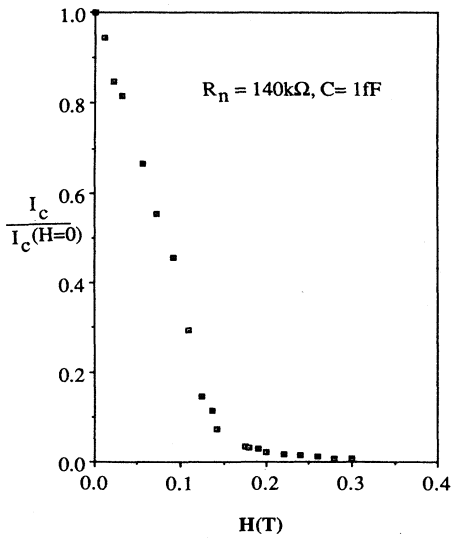

FIG. 10. I_c vs H for the sample with $R_n = 140$ kΩ. The critical currents are normalized to the value in zero magnetic field.

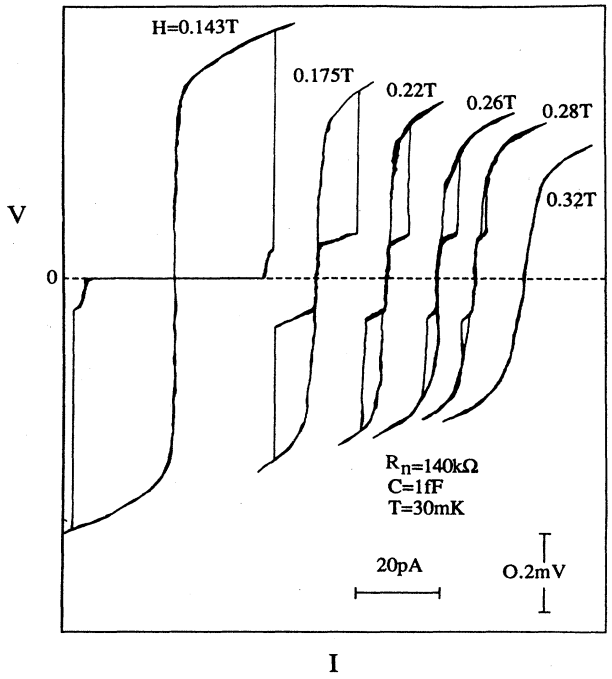

FIG. 11. Series of I-V curves taken as a function of magnetic field at fixed temperature, for the sample with $R_n = 140$ kΩ.

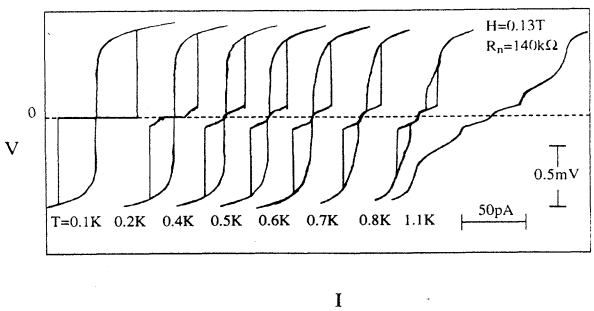

FIG. 12. Series of I-V curves taken as a function of temperature at fixed magnetic field, for the sample with $R_n = 140$ kΩ.

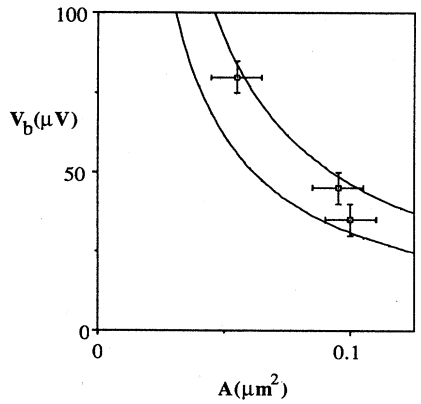

FIG. 13. Measured blockade voltage V_b as a function of junction area. The three measured samples (from left to right) had $R_n = 140$, 35, and 15 kΩ. The curves correspond to $e/2C$, calculated using an oxide barrier thickness of 30 Å (top curve) and 20 Å (bottom curve), and $\epsilon_r = 6$.

tive at $I < I_c$, as described in the previous section, beyond a critical field H_t (~ 0.16 T, in Fig. 11) the whole character of the I-V curve changes. The response now becomes *highly* resistive at low currents (with dynamic resistance of order R_L), rising to a plateau at $V \equiv V_b$. If the current is increased further, the voltage rises on a ramp with slope $R \sim 10^6$ Ω, from which it jumps to the gap voltage V_g at a current value we identify as I_c. Once the novel behavior sets in, the value of V_b is found to be insensitive to magnetic field and temperature. This is shown, for example, in Fig. 12: The I-V curves, taken at the intermediate field of 0.13 T as a function of temperature, undergo a transition similar to that shown in Fig. 11 as a function of field. Apart from rounding, the value of V_b is the same in all cases.

By reducing the Josephson coupling energy with magnetic field or temperature, we can thus induce a striking transition in the shape of the I-V curve. The new curves are highly resistive at low currents, qualitatively reminiscent of the Coulomb blockade effect mentioned in the Introduction. Moreover, as shown in Fig. 13, to the precision with which C_i is known, the measured V_b corresponds to $e/2C_i$ in all measured samples, where C_i is the *intrinsic* capacitance. In this novel regime, features typical of the Coulomb blockade, such as the knee at $V \approx e/2C$, coexist with a sharp voltage jump at a current reminiscent of the Josephson critical current I_c.

III. THEORETICAL MODELS AND DISCUSSION

We now present our interpretation of the experimental results. We begin with a simple discussion of the assumptions involved in applying the resistively and capacitively shunted junction (RCSJ) model to our devices. We then discuss a few familiar examples in which the RCSJ model has been used in the past to explain the behavior of conventional (high capacitance, high E_J) Josephson junctions. This discussion is used as the springboard for the interpretation of our novel experimental results. Sections III B–III D contain the heart of our theoretical treatment. Section III B considers the implications of the RCSJ model in the semiclassical limit, when the Josephson and thermal energies are comparable. This treatment is used to provide estimates for our experimental results in the higher-temperature regime, when quantum fluctuations are small compared to thermal fluctuations. In Secs. III C and III D we discuss a quantum-mechanical treatment of the problem, and for simplicity ignore (for the most part) thermal fluctuations. This approach is expected to be relevant at low temperatures, as thermal effects freeze out.

A. The base model

1. Assumptions

The discussion presented in this article is based on the usual resistively and capacitively shunted Josephson junction (RCSJ) model[19,20] shown schematically in Fig. 14. A complete description of the model involves characterizations of the Josephson coupling channel by a definition of E_J, of the capacitive channel by the definition of C, and of the dissipative channel by the definition of $R(V)$.

We assume that E_J is given by $E_J = \hbar I_{c0}/2e$, where I_{c0} is given by the Ambegaokar-Baratoff relation:[18]

$$I_{c0} = \frac{\pi\Delta}{2eR_n}\tanh\left[\frac{\Delta}{2k_BT}\right] . \tag{3}$$

This formula has been found to give excellent agreement with critical current measurements on large low-resistance ($R_n < 5$ Ω) Sn–Sn oxide–Sn junctions where thermal and quantum fluctuations effects are expected to be negligible.[15] These samples are fabricated in this lab with the same equipment and techniques as those used in the fabrication of the small high-resistance samples which are the subject of this study.

We also assume that C can be approximated by the intrinsic capacitance C_i and that the relevant resistance is given by R_L for $|V| < 2\Delta/e$, and by R_n otherwise. While it may seem surprising that the extensive distributed capacitance of the leads does not overwhelm the small intrinsic capacitance, there is significant experimental

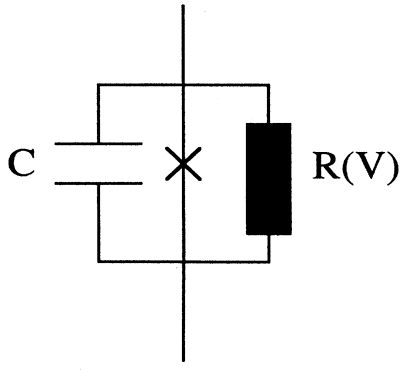

FIG. 14. Schematic of the equivalent junction circuit used in the RCSJ model.

justification for our assumption. For example, van Bentum *et al.*[9] and Hartmann *et al.*[10] recently performed Coulomb blockade measurements in a scanning tunneling microscope (STM) with normal electrodes: Their measured capacitance values in the neighborhood of 10^{-18} F were unaffected by the very large distributed capacitance of the STM apparatus.

To further test the effect of lead impedance on the dynamics of our devices, we have fabricated junctions in single, double, and 11-junction configurations. The behavior of the smallest junction in each of the measured configurations appeared mostly unaffected by the presence of companion junctions in the leads, whose capacitance and inductance would grossly affect the lead impedance. Thus it appears that the dynamics of our junctions depend mainly on their *intrinsic* impedance. While this is in apparent contrast with the observations of Martinis *et al.*[21] on much larger junctions, we believe that the different behavior may be due to the importance of *single*-electron effects in our devices. As the energy change due to the tunneling of a single electron becomes dominant, the problem will become more microscopic in nature, and the time scale fast. The time scale for the dynamics of a conventional semiclassical Josephson junction (of the kind used by Martinis *et al.*[21]) is given by the Josephson plasma frequency, typically of order 10^9–10^{11} Hz. In the opposite regime, when the charging energy is completely dominant (as is the case in the observation of van Bentum *et al.*[9]), the characteristic frequency is thought to be the inverse of the electron tunneling time, typically of order 10^{15} Hz. The faster the time scale the higher the impedance of the inductive leads. These arguments do not show that the devices will be *completely* independent of the leads; we believe, however, that the parasitic contributions are small, and that the intrinsic capacitance C_i, in our system, is a reasonable estimate of the total capacitance of the device. This position will be further justified *a posteriori* by comparing the predictions of this model with our data.

Finally, since we believe that the low-temperature behavior of our devices is not dominated by dissipation in the leads, it is important to consider the nature of the intrinsic dissipation $R(V)$. Since dissipation in an ideal Josephson device is determined by the tunneling of quasiparticles, the discrete nature of the charge transfer in the tunneling process will become important. We consider this especially in the last sections of this paper, when we analyze the coexistence of the Coulomb blockade with some features of Josephson tunneling. One interesting aspect of our measurements of R_L, the low-voltage part of $R(V)$, is that its temperature dependence follows quasiparticle thermal activation at higher temperatures, but flattens off at low T, as described by (2). We believe that the existence of a finite R_L as $T\rightarrow 0$ is not due to metallic whiskers partially shorting out the barrier, since $R_L(0)$ is very large, typically of order 10^8 Ω. The whisker's maximum length would have to be of order the barrier thickness (≈ 25 Å). Therefore, a resistance of 10^8 Ω would require a resistivity much larger than 1 Ω cm, even for a diameter as small as one atomic spacing. This appears unlikely, and we believe that this temperature-independent dissipation term may instead be due to a tunneling mechanism.

The apparent proportionality of the residual leakage resistance to R_n^2 (see Fig. 9), suggests that a possible source of low-T dissipation may reside in the effect of Andreev reflections on the tunneling I-V response. This was analyzed by Blonder, Tinkham, and Klapwijk (BTK),[22] who showed that the Andreev channel should have a probability going as the square of the probability of charge transfer in the normal channel. If we extrapolate the square-law relationship back, we find that $R_n \approx R_L(0)$ for a resistance of order 100 Ω. In the BTK theory, the point at which the normal and leakage resistance are approximately equal corresponds to a device of "barrier strength" Z (see Ref. 22) of order one, i.e., a device whose barrier is very weak, and whose I-V characteristic begins to resemble a microbridge rather than a tunnel junction. A resistance of 100 Ω appears high for a device with microbridge characteristics. However, this apparent inconsistency can be resolved if we remember that there is evidence (from the magnetic field data, for example) that the oxide barrier may be quite nonuniform. Since the Andreev term is proportional to the *square* of the tunneling probability, a small fraction of the junction with a thinner barrier may dominate in the leakage term.

2. *Basic consequences*

The nondissipative aspect of the RCSJ model can be described by the Hamiltonian

$$H=-E_J\cos\phi+Q^2/2C\ .$$

Taking account of the quantum nature of the phase-number relationship described by the commutator $[\phi,Q]=2ie$, by making the operator replacement $Q\rightarrow 2ie\,\partial/\partial\phi$, we obtain

$$H=-E_J\cos\phi-4E_c\partial^2/\partial\phi^2\ , \tag{4}$$

where, again, $E_c=e^2/2C$. Leggett and other authors[23–27] have shown how to introduce damping into the problem by coupling an infinite collection of harmonic oscillators (representing the environment) to the system described by (4).

In the classical approximation, $E_c \ll E_J$, and one can neglect the term in $\partial^2/\partial\phi^2$. Thus, in the ground state, $\psi(\phi)$ is approximated by a delta function at the minimum ($\phi=0$) of the Josephson cosine potential [more exactly, the width $\delta\phi\approx(E_c/E_J)^{1/4}$]. Introducing a current bias by adding a term $-(\hbar/2e)I\phi$ to (4) (the "tilted washboard model"), the minimum energy shifts to

$$\phi=\sin^{-1}(I/I_{c0})$$

so that $I=I_{c0}\sin\phi$, the usual Josephson current relation. However, when $I>I_{c0}$, there is no energy minimum, and the representative point accelerates down the washboard, reaching a terminal velocity $\dot{\phi}$ (corresponding to a voltage $V=\hbar\dot{\phi}/2e\approx 2\Delta/e$) limited by dissipation due to quasiparticle transfer at the gap voltage. Thus the model described by (4) leads in this limit to the monotonically increasing $I_c=I_{c0}(T)$, and $R_0=0$, since $V=0$ for $I<I_c$.

These results well describe the behavior of conventional large-area low-resistance (high I_{c0}) junctions; the I-V curves of such devices, in which $E_J \gg E_c, k_B T$, were described in the Introduction.

If $k_B T$ or E_c are significant in comparison with E_J, $I_c(T)$ is no longer expected to closely follow $I_{c0}(T)$. It is now well established, both experimentally[28–32] and theoretically,[33–38] that thermally activated "escape" from the minimum of the tilted cosine potential causes "premature switching" to the finite-voltage regime. The thermal escape rate is approximately given by

$$\frac{1}{\tau} = \nu_a e^{-\Delta U(I)/k_B T} .$$

The attempt frequency is given approximately by $\nu_a \approx \omega_p / 2\pi$, and is typically of order 10^{10} Hz $[\omega_p = (1/\hbar)(8 E_J E_c)^{1/2}]$. As a result, in experiments with current sweep times of order 1 s, escape will occur as soon as $\Delta U(I)/k_B T \approx \ln \nu_p \approx 20 \gg 1$. Taking account of the fact that $\Delta U(I) \approx 2E_J(1 - I/I_{c0})^{3/2}$ to a good approximation, one expects switching to occur when this $\Delta U(I) \approx 20\, k_B T$, or more generally, at

$$I_c = I_{c0}\left\{1 - \left[\frac{k_B T}{2E_J} \ln\left[\frac{\nu_p \delta I_c}{dI/dt}\right]\right]^{2/3}\right\}, \tag{5}$$

where $\delta I_c/(dI/dt)$ is the time spent sweeping through the switching distribution. A more careful analysis by Danchi *et al.*[31] gives the same result, apart from small numerical refinements. Thus the apparent I_c depends logarithmically on the current sweep rate.

Because this escape is a probabilistic event, the I_c measured in an actual experiment is different on each current sweep. The distribution of measured I_c values has a characteristic width δI_c, mentioned above, which is proportional to the extent of the depression of I_c. For the dependences cited above, one finds

$$\delta I_c = \frac{2}{3} \frac{I_{c0} - I_c}{\ln[\nu_p \delta I_c/(dI/dt)]} . \tag{6}$$

In our samples, $I_c \sim 0.1 I_{c0}$ and the logarithm is of order 20, so that (6) would give $\delta I_c \approx 0.03 I_{c0}$. This result is inconsistent by an order of magnitude with the new data, in which $\delta I_c = 0.003 I_{c0}$. The switching distribution is simply too narrow to be compatible with an explanation of the depression of the observed I_c so far below I_{c0} by premature switching. Put another way, for I so far below I_{c0}, the cosine potential is barely tilted, and the height of the barrier is almost independent of current. Hence a small change in current could hardly account for a sudden onset of switching out of the zero-voltage state. Moreover, this picture of stochastic escape is qualitatively incompatible with the finite voltage below I_c, which implies a steady-state phase evolution, rather than metastable locking in position in a single well until the escape.

As one goes down in temperature, eventually this thermally activated escape becomes less likely than escape by macroscopic quantum tunneling (MQT) through the barrier.[21,23,25,26,39–44] This mechanism already takes us beyond the classical regime, but in the junctions studied previously,[21,39–44] this escape probability was sufficiently low that one could still treat the phase as a rather localized semiclassical quantity, which occasionally made a probabilistic transition through the barrier into a free-running finite-voltage state. In this regime, it was shown that there is a crossover temperature given roughly by[45]

$$k_B T_{\text{crossover}} \approx \hbar \omega_p / 2\pi = (8 E_c E_J)^{1/2}/2\pi . \tag{7}$$

Below this temperature, the same qualitative probabilistic switching should occur as in the thermally activated regime, except that the constant $T_{\text{crossover}}$ replaces the actual temperature. Thus the same inconsistency between a narrow switching distribution and a huge depression of I_c below I_{c0} exists in this regime as in the thermally activated one, and a more appropriate explanation must be found.

B. The new regime: the semiclassical limit

In the previous section, we have argued that the usual dynamics describing Josephson junction behavior do not apply to our observations. The common situation of a constant ϕ value at $I < I_c$ followed by a probabilistic switching into the finite-voltage "running" state is simply inconsistent with our measurements. Since the observed I-V curves are resistive, even at the lowest currents, it seems very plausible that the dynamics of the system are characterized by very frequent phase slips, which would give rise to dissipation, and thus to R_0. Mechanisms of these frequent phase slips would be thermal activation (since for devices typical heights of the Josephson potential are of order 1 K), and quantum tunneling (since E_c is of order E_J). However, since a current bias tilts the Josephson potential, the system would possibly exhibit no critical current at all, since once the first phase slip occurs the subsequent ones become easier. To account for the observations, therefore, we need to consider the effect of damping as a retrapping mechanism. Qualitatively, therefore, the dynamics of our devices may be described as follows: At $I < I_c$, the phase frequently escapes from its potential well. The energy it acquires in a 2π phase slip, however, is lost through damping, and the phase retraps in a subsequent well. This process goes on until $I = I_c$, at which point one of two things happens. Either the potential tilt becomes enough for the system to acquire more energy than it loses from damping, or some intrinsic limit to the maximum Josephson current is exceeded. We believe the first situation to be valid at higher temperatures, in what we call the "semiclassical regime," and the second situation to be valid at low temperatures, in what we call the "quantum regime."

1. *Estimates for the critical current: effect of damping*

It is well known that so long as a junction is underdamped, the amount of damping affects the escape rate only through a modest change in the prefactor in (4). Since this factor only enters logarithmically in the depression of I_c, this change is usually unimportant. However, the amount of damping is the *crucial* factor in

determining the retrapping critical current I_r. Because I_c and I_r coincide above about $\frac{2}{3}T_c$ in the new data, where they are both strongly reentrant, it is appropriate to review the physics of what is going on with I_r as well as I_c.

Within the simple RCSJ approximation, in which the damping is attributed to a simple linear resistor of value R shunting the junction, Stewart[18] and McCumber[19] showed that the degree of damping was conveniently described by the dimensionless parameter

$$\beta_c = \frac{2eI_{c0}R^2C}{\hbar} .$$

They worked out the dependence of I_r/I_{c0} on β_c, and in particular showed that so long as β_c was significantly larger than unity, the relation was the simple one

$$\frac{I_r}{I_{c0}} = \frac{4}{\pi}\frac{1}{\sqrt{\beta_c}} . \tag{8}$$

From these relations it follows that

$$I_r \propto [I_{c0}(T)/C]^{1/2}R(T)^{-1} . \tag{9}$$

The temperature dependence of I_{c0} is the well-known Ambegaokar-Baratoff relation (3), which monotonically increases as T is decreased. Accordingly, if (9) is to describe the temperature dependence of I_r in this reentrant regime below $\sim 0.9T_c$, it must result from the temperature dependence of $R(T)$. In fact, if we substitute the leakage resistance approximated by (2), we find excellent agreement with the *shape* of the temperature dependence, as shown in Fig. 5(b). (The magnitude is too small by a factor ≈ 7, but we shall see that the discrepancy can be accounted for largely by fluctuation effects which are not included in the Stewart-McCumber analysis.)

To see whether it is reasonable to substitute R_L for R in β_c, it is necessary to examine the physics behind this formula for I_r. It is useful to consider the motion of a representative point in the tilted washboard potential (see Fig. 15). In the absence of damping, it moves horizontally, representing the conservation of energy in the presence of the energy input from the current source. In the presence of damping, the trajectory sags downward to reflect the loss of energy at the rate $dE/dt = -V^2/R$. From the Josephson relation, V is related to the rate of change of phase along the washboard by $V = (\hbar/2e)d\phi/dt$, as well as the component of the total energy E stored in the capacitance, $\frac{1}{2}CV^2$. By combining these relations, one can write

$$\frac{dE}{d\phi} = -\frac{\hbar}{2eR}\left[\frac{2(E + E_J\cos\phi)}{C}\right]^{1/2} ,$$

in which R is to be understood as being a function of the instantaneous voltage, which is determined by integrating this equation forward in ϕ. The condition for I_r is that, if the representative point starts at the top of one maximum of the tilted washboard, where it has zero velocity, it should just exactly reach the next maximum, again with zero velocity. If the tilt (i.e., current I) is any greater, the representative point will run away at a rate limited by the damping; if it is any less, it will be trapped in the next minimum. For this critical trajectory, the voltage oscillates between zero (at the maximum) and a maximum value such that $\frac{1}{2}CV^2 \cong 2E_J$, corresponding essentially to the plasma frequency. The *average* voltage, as read off the I-V curve, is evidentally less than $2\Delta/e$. Theoretically, one expects the quasiparticle conductance to be only weakly dependent on voltage for $eV < 2\Delta$. Accordingly, it is plausible that the *average* R determining I_r should be quite similar to the *measured* R_L at the *average* voltage, and that is what the data imply.

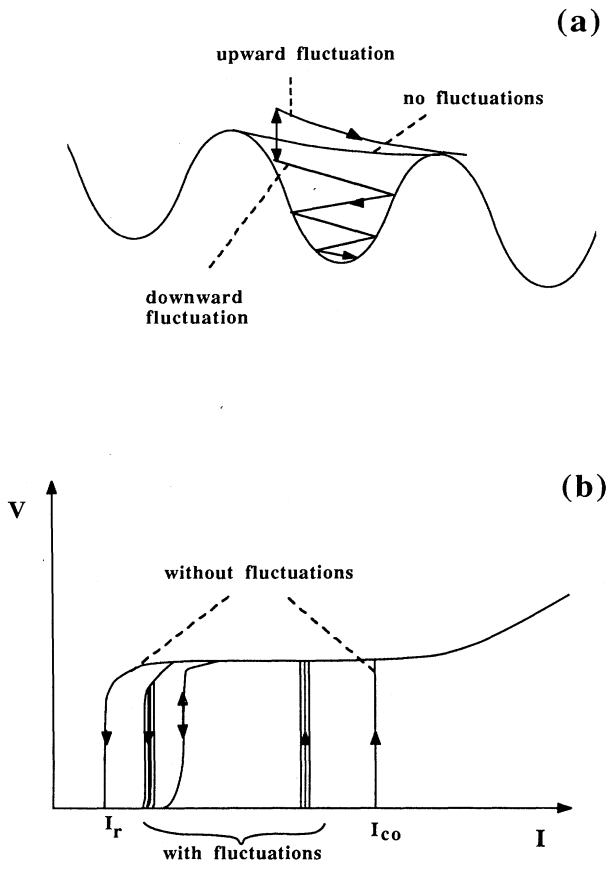

FIG. 15. (a) Schematic of the effect of fluctuations on the retrapping process. Total system energy is plotted vs phase. (b) Sketch of the effect of thermal fluctuations in reducing and eventually eliminating the hysteresis in an underdamped Josephson junction.

2. *Estimates for the critical current: effect of thermal fluctuations*

It is well known, as noted above, that thermal fluctuations have the effect of reducing the measured I_c by inducing premature switching out of the zero-voltage state. It is less well known that thermal fluctuations have the opposite effect on I_r, i.e., they *increase* it. This point has been made by various authors, recently by Cristiano and Silvestrini (CS),[46,47] who also presented the results of numerical calculations. Since this result seems counterintuitive to many, it is worthwhile to give a simple physical

argument which establishes the correctness of the sign of the effect.

Consider Fig. 15(a), which depicts the tilted washboard potential at the current corresponding to I_r in the absence of fluctuations. At this current value, the representative point starting at the top of one barrier follows a trajectory which reaches the corresponding point at the next maximum. Now consider the effect of fluctuations which raise or lower the energy discontinuously at some point on this trajectory. If the initial fluctuation is downward, the trajectory continues downward because energy is dissipated at the rate $-V^2/R$ and is not recovered from the current drive since the trajectory is confined to a single minimum. On the other hand, if the initial fluctuation is upward in energy, this increases $\frac{1}{2}CV^2$ and hence V^2/R, so that the trajectory falls more steeply, eventually returning to the marginal trajectory on which it started, which it follows stably until the next fluctuation occurs. Since upward fluctuations recover while downward ones cause retrapping, it is clear that the fluctuations tend to make the system *more* stable against runaway. Accordingly, the marginal current value (tilt) giving retrapping is *greater* in the presence of fluctuations than without them, so I_r is *increased.*

As shown schematically in Fig. 15(b), then, the effect of fluctuations is to induce a convergence of I_r and I_c toward a common intermediate value, eliminating hysteresis. Another effect of the fluctuations is to cause both I_r and I_c to acquire a probabilistic switching character, as has been mentioned earlier. As the fluctuations increase further in strength beyond that causing the coalescence of I_c and I_r, the switching back and forth in the vicinity of this critical current value becomes so rapid compared to experimental time scales that the measured voltage averages to give a smooth continuous resistive transition. The value of this coalesced $I_c = I_r$ can be determined by simulation methods, but one can also reason that it will be determined by the physics of I_r rather than the physics of I_c, since when fluctuations are this prominent, the system is activated out of its metastable minima so quickly that "premature" switching is taking place continuously. The crucial question is at what current the damping assisted by fluctuations leads to the retrapped state being the more dynamically stable one, and this is the consideration determining I_r. We conclude that, in the nonhysteretic regime near T_c where fluctuations are dominant, *the measured critical current I_c should be interpreted as I_r* as enhanced above the value given by (8) by the presence of fluctuations. This theoretical conclusion is confirmed by the experimental observation (see Fig. 5) that the temperature-dependence trend set by the coalesced $I_r = I_c$ in the nonhysteretic region continues as that of I_r when the junction becomes hysteretic.

With the principle established that the trapping mechanism (including the major enhancement by fluctuations) determines not only I_r at all temperatures but also I_c above the temperature at which hysteresis disappears, we now must estimate how large is the enhancement of (8) by fluctuations. The results of CS are restricted to values of $\gamma = 2E_J/kT = 5-50$ and attempt numbers $\approx 10^3-10^5$, whereas in our samples γ is typically less than 1 and the attempt numbers are of order 10^{10}. Still, we can use their results by noting that they show that the enhancement of I_r increases approximately linearly in the logarithms of both γ and L. Using this observation, if one extrapolates their results to $\gamma \leq 1$ and $L \approx 10^{10}$, one estimates an enhancement factor of roughly 5 or greater; for comparison, the largest enhancement for the parameters considered by CS is about 3, so this extrapolation is not terribly extensive. It is reassuring, nonetheless, that our direct simulations also give enhancements by similar factors. Since it appears that the enhancement factor should not depend strongly on γ so long as it is less than or of order unity, nor on L so long as it is within an order of magnitude of 10^{10}, we conclude that the temperature dependence of the observed I_r should be very similar to that of the unfluctuated result (8), but that the magnitude should be larger by a factor of order 5 because of the fluctuations. Considering the uncertainties in parameter values (especially C) and in this extrapolation, this estimate is quite consistent with the observation that the measured I_r is roughly 6–7 times the value given by (8), and has essentially the same temperature dependence.

3. *The low-voltage dissipative branch: R_0*

Another interesting feature of our observations is the presence of a resistive state at currents below the measured I_c. At higher temperatures, the I-V curve is not hysteretic, and the presence of a dissipative branch is not surprising. We have seen that damping appears to play a key role in the determination of the critical current in this regime. We believe that the observation of a nonzero R_0 is also primarily due to damping.

For almost all our junctions, at temperatures above 1 K, thermal fluctuations are very large compared to the Josephson coupling energy. The escape out of the Josephson potential well is thus very rapid, with rates of the order of the Josephson plasma frequency ω_p. The "phase point" is thus constantly out of the Josephson potential well, and gradually slips downhill. At currents less than the retrapping current I_r, however, the escape of the phase point over many wells is not energetically favorable: It loses energy through dissipation faster than it gains energy from the motion downhill. The phase point will thus retrap in a subsequent well.

It would be desirable to compare the observed values of R_0 with estimates extracted from theoretical calculations of the rates of escape out of the Josephson potential. Unfortunately standard theoretical estimates for the escape rate out of a metastable potential appear to break down when k_BT becomes greater than barrier height. Moreover, we cannot interpret our low-temperature data in this fashion, since below 1 K we expect quantum tunneling to be very important. Our comparison with accepted thermal-activated escape theories is thus limited; we can only expect quantitative agreement from our lowest-resistance sample ($R_n = 550\ \Omega$, $E_J \approx 45$ K), for which the Josephson coupling energy is reasonably large compared to k_BT even at relatively high temperatures. For this sample, at temperatures above 2 K, the contribu-

tion of quantum tunneling should be minor, but the ratio of E_J to $k_B T$ is still large.

As we point out above, the existence of substantial resistive voltage even for $I \ll I_c$ indicates that the phase variable is steadily evolving in time, at an average rate $d\phi/dt = 2eV/\hbar$. In the presence of a current, the successive minima drop in energy by $hI/2e$, and the barrier heights for escape in the uphill and downhill directions are shifted by $\pm hI/4e$ with respect to the zero-current case. As a result the escape probability is greater in the downhill direction than in the uphill one, and there is a *net* rate of downhill tunneling proportional to I (for small I). Hence there is a voltage $V \propto d\phi/dt \propto I$, which can be described by the resistance $R_0 = V/I$. We assume that the system will lose energy by dissipation and retrap in the adjacent well, making the phase slip per activation event approximately equal to 2π at low current.

We now need to calculate the difference between uphill and downhill escape rates. We define Γ^+ to be the escape rate to the right (downhill) and Γ^- to be the value of the escape rate to the left. Expanding around $I = 0$ the following estimate is obtained:

$$R_0 = \frac{\hbar}{2e}\frac{1}{I}\frac{d\phi}{dt} \approx \frac{\hbar}{2e}\frac{1}{I}2\pi(\Gamma^+ - \Gamma^-) . \tag{10a}$$

To estimate the escape rates we assume that Γ^+ and Γ^- are independent, i.e., we assume that Γ^+ is only dependent on the barrier height to the right, and not affected by the fact that escape to the left is also possible. Γ^+ and Γ^- can then be estimated by using results from thermal-activated-escape theories. They are a function of the uphill and downhill barrier heights, respectively, and the resistance and capacitance of the device. For the parameters of our lowest-resistance junction ($R_n = 550\ \Omega$), the differences in the estimates for the theories by Kramers,[33] Büttiker, Harris, and Landauer,[37] and Barone, Cristiano, and Silvestrini[38] are small. We use the last approach for our actual estimates since it is valid closer to the breakdown at $E_J \approx k_B T$. The escape rate is thus given by[38]

$$\Gamma = \frac{1}{RC}\sum_{n=1}^{\infty}\frac{1}{n!n}\left[\left[\frac{\gamma U_0}{2}\right]^n - \left[\frac{\gamma E_0}{2}\right]^n\right] , \tag{10b}$$

where U_0 is the barrier height (in the uphill or downhill direction) and E_0 is the initial energy of the representative phase point, both normalized to E_J, while $\gamma = 2E_J/k_B T$. E_0 is not a well-known parameter for the system: However, it is reasonable[38] in the large γ limit to assume that $E_0 \approx 2/\gamma$, which corresponds to the particle having initial energy equal to $k_B T$. For large γ, therefore, E_0 is small, and (10b) is easily applied.

Using (10a) and (10b), we can now estimate the low-current resistance R_0 for our lowest-resistance (largest γ) sample. The agreement is excellent, as shown in the Arrhenius plot of Fig. 16, using the estimated *intrinsic* capacitance C_i, the leakage resistance given by (2), and no adjustable parameters. We can use the same approach to estimate R_0 for higher resistance (lower γ) samples. However, (10b) becomes much more sensitive to E_0, and the approach only works as an order-of-magnitude estimate.

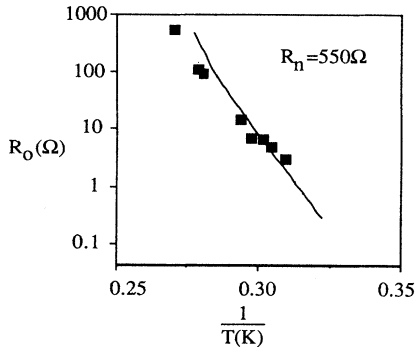

FIG. 16. R_0 vs T^{-1} for the sample with $R_n = 550\ \Omega$. The line is a theoretical fit with no adjustable parameters using theory outlined in the text [see (10a) and (10b)].

For our higher resistance samples, standard models of thermally activated escape no longer apply. For the sample with $R_n = 140\ \text{k}\Omega$, for example, the Josephson coupling energy E_J only corresponds to 0.3 K. Except at the lowest temperatures, the representative phase point is constantly thermally activated out of the potential well. The motion of the phase point, therefore, might resemble more a diffusive random walk, than a sequence of well-defined activated jumps from well to well. Unfortunately, to our knowledge, this regime has not yet received extensive theoretical scrutiny in the underdamped case. To obtain a simple phenomenological prediction, we assume

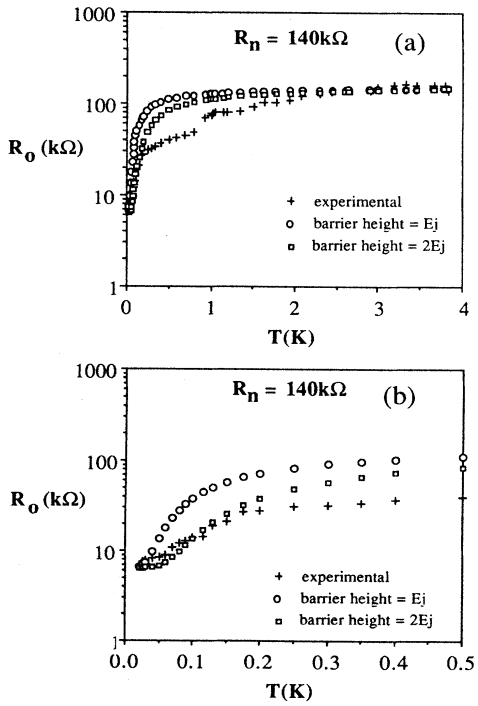

FIG. 17. Comparison of experimental and model dependence of R_0 vs T for the sample with $R_n = 140\ \text{k}\Omega$. The horizontal scale is expanded in (b).

that the rate of motion downhill is proportional to the amount of time the system spends above the barrier. The proportionality constant must deduce to R_n as $T \rightarrow T_c$. We write

$$R_0 = R_{\rm qtm} + (R_n - R_{\rm qtm}) e^{-\Delta U/k_B T} , \tag{11}$$

where $R_{\rm qtm}$ is the contribution of quantum tunneling, estimated below in Sec. III C. The activation energy ΔU, given by the barrier height $\sim 2E_J$ in a classical treatment, may be reduced in a more complete quantum treatment, since part of the Josephson potential well is below the lowest quantum state. This rough phenomenological estimate is good enough to give an order-of-magnitude estimate and an idea of the general trend of the data, as shown in Fig. 17, where $R_{\rm qtm}$ was chosen to fit the limit as $T \rightarrow 0$. A more complete treatment will be required for quantitative agreement.

4. *First conclusions*

From the above, we conclude that the semiclassical model can account for the entire $I_r(T)$ and for the $I_c(T)$ (and R_0, qualitatively) in the nonhysteretic temperature range, provided the following.

(a) The effective capacitance in the RCSJ model has a value $\approx 1-2$ fF, as estimated from the geometry with little allowance for capacitance contributed by the leads.

(b) The temperature-dependent damping is governed (at least in the frequency range relevant to I_r) by the leakage resistance (2), which agrees with the measured value of R_L.

(c) Thermal fluctuation effects enhance the I_r given by (8) by a factor of order 5, as expected from simulations.

However, the semiclassical model *cannot* account for the low-temperature data, where $I_c > I_r$, with a measurable resistive voltage at all current levels, including $I < I_c$. The possibility that quantum effects provide the explanation is suggested by the fact that for $C \approx 1$ fF, as found above, the Coulomb charging energy $E_c = e^2/2C \approx 1$ K, which is comparable with E_J. In the next section, we will explore this possibility.

C. The quantum limit: ϕ-space description

In Sec. III B we have given a phenomenological classical treatment of the behavior of a Josephson junction when E_J is of order $k_B T$. In our devices, however, the estimated charging energy is also of order the Josephson coupling energy, causing very large quantum phase uncertainties. Therefore, to understand our measurements, especially as thermal fluctuations freeze out for $T < 1$ K, it is necessary to extend our treatment to include the quantum-mechanical nature of the phase. We begin in this section by treating the problem in ϕ space, and continue in Sec. III D by looking at the conjugate representation in Q space. While the former representation is a natural extension of the classical treatment presented above, the Q-space approach should be more appropriate in the extreme quantum limit ($E_c > E_J$), in which uncertainties in ϕ become comparable to the well spacing in the Josephson potential (2π).

1. *Nature of the quantum ground state*

Recalling the form of the full Hamiltonian (in the absence of a current) given above as (3), namely,

$$H = -E_J \cos\phi - 4E_c \partial^2/\partial\phi^2 , \tag{12}$$

we see that the parameter $x \equiv E_c/E_J$ provides a measure of the relative importance of the charging energy in forcing a delocalization of the phase, away from the minimum potential energy point at $\phi = 0$. Physically, this reflects the uncertainty relation between phase and particle number (or charge):

$$\Delta\phi \, \Delta N \geq 1 .$$

For $x \ll 1$, as noted above, the ground state is a narrowly peaked wave function $\psi(\phi)$ with width of order $x^{1/4}$, and there are many higher states in each minimum, resembling the excited states of a harmonic oscillator. By contrast, when $x \gg 1$, the term in E_c is dominant, and ψ approaches a constant to minimize it. At this point, one can no longer ignore the periodicity of the potential term $-E_J \cos\phi$ and the question of whether ϕ should be viewed as an extended variable or a cyclic one such that ϕ and $\phi + 2\pi$ (or 4π, if we include quasiparticles[27]) are physically indistingushable. From the former point of view, $\psi(\phi)$ has the form of a Bloch function $u(\phi)e^{iq\phi}$, where $u(\phi)$ is periodic with period 2π; from the latter point of view, $\psi(\phi)$ is only defined between $-\pi$ and $+\pi$, and it must satisfy appropriate boundary conditions at those points. So long as we restrict our attention to the ground state, which we expect to correspond to $q = 0$ in the Bloch picture, and to the boundary conditions $\psi(\pi) = \psi(-\pi)$ and $\psi'(\pi) = \psi'(-\pi) = 0$ in the single-cell picture, both pictures yield the same eigenvalue problem, and the same energy eigenvalue E.

Since this problem is one-dimensional, it is easy to solve by numerical means. However, one gets a bit more insight by a variational approach, using trial functions appropriate to the limiting cases of $x \ll 1$ and $x \gg 1$, respectively. For $x \ll 1$, one assumes a Gaussian trial function,

$$\psi(\phi) \sim e^{-\phi^2/4\sigma^2} , \tag{13}$$

where σ, the rms spread in ϕ, is chosen to minimize the expectation value of (12). The resulting minimum energy is

$$E = -E_J e^{-\sigma^2/2}(1 - \sigma^2/2) , \tag{14a}$$

where σ has the value determined by the solution of the transcendental equation

$$\sigma^4 e^{-\sigma^2/2} = 2x . \tag{14b}$$

For $x \ll 1$, (14) leads to the analytic approximation

$$E = -E_J[1 - (2x)^{1/2}] . \tag{14c}$$

In the other limiting case of $x \gg 1$, an appropriate trial function which satisfies the boundary conditions at the edge of the cell is

$$\psi(\phi) \sim (1 + a\cos\phi) . \tag{15}$$

Minimization of the expectation value of the energy with respect to the parameter a leads to the condition that

$$a = 4x\,[(1+1/8x^2)^{1/2}-1]\,. \tag{16a}$$

For this value of a, the energy is

$$E = -E_J 2x\,[(1+1/8x^2)^{1/2}-1]\,. \tag{16b}$$

For $x \gg 1$, this has the limiting form

$$E \approx -E_J/8x = -E_J^2/8E_c\,, \tag{16c}$$

where the second form shows explicitly that in this limit the binding energy is *second order* in E_J, in contrast to the *first-order* binding energy in the usual other limit (14).

These variational approximations to the ground-state energy are plotted in Fig. 18(a). The tight-binding approximation (13) gives a lower (more accurate) energy for $x < \frac{1}{4}$, and the weak-binding approximation (15) gives a better energy for $x > \frac{1}{4}$. Numerical solutions in the crossover region near $x = \frac{1}{4}$ show that the exact binding energy exceeds the better of the two approximations by less than 5%, even in the worst case. The wave functions $\psi(\phi)$ for values of x ranging from 0.05 to 1 are shown in Fig. 18(b). In this figure, the loose-binding approximation is shown for $x > \frac{1}{4}$ and the tight-binding approximation for $x < \frac{1}{4}$. Qualitatively, it is clear that for $x > \frac{1}{4}$, the probability density for the phase variable ϕ is sufficiently delocalized that it is no longer a good approximation to

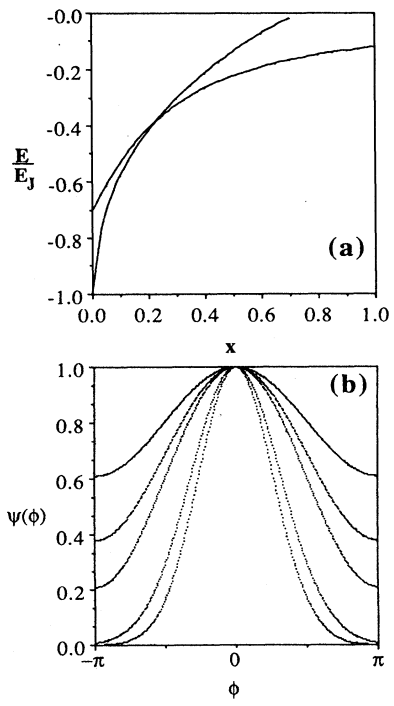

FIG. 18. (a) Estimated binding energy E vs $x = E_c/E_J$. The two curves correspond to two different trial wave functions, as outlined in the text. (b) Estimated ground-state wave function $\psi(\phi)$ as a function of ϕ, for different values of x. From top to bottom the curves correspond to $x = 1, 0.5, 0.3, 0.1, 0.05$.

treat ϕ as a semiclassical variable as in the discussion of the foregoing sections of this paper.

We now will investigate to what extent quantum effects resulting from going beyond the semiclassical approximation can account for the puzzling low-temperature data cited above.

2. *Interpretation of the resistance R_0*

Our treatment of this problem in the quantum regime is quite similar to that given in Sec. III B, for the classical case. For the lower-voltage branch of the I-V curve, at $I < I_c$, the expectation value of the phase tunnels from well to well, evolving in time at a rate $d\phi/dt = 2eV/\hbar$. To develop an interpretation of this voltage in the ϕ-space framework, we assume that the degree of delocalization is sufficiently small that we can reasonably represent $\psi(\phi,t)$ by a function localized in one well, which occasionally tunnels into an *adjacent* well. (For the present, we assume $T=0$, so there are no thermally activated hops.) In the presence of a current, the tunneling probability is greater in the downhill direction than in the uphill one, and there is a *net* rate of downhill tunneling proportional to I (for small I). Hence there is a voltage $V \propto d\phi/dt \propto I$, which can be described by the resistance $R_0 = V/I$. While perhaps *qualitatively* appropriate for all samples, this picture can only be expected to be *quantitatively* correct for the samples with $x < 1$, so that the phase uncertainty is still not large compared to 2π. The sample with $R_n = 14.8\ \text{k}\Omega$, and $x \approx 0.25$ thus appears to be a good example for testing the accuracy of this model.

We implicitly assume that there is sufficient damping present that, after each tunneling event, the system equilibrates into the lowest quantum state in the well into which it has just tunneled, before tunneling again. If the system did *not* lose energy in this way, it would run away, since in successive wells (in the downhill direction) it would experience lower and lower barriers, and tunnel ever more readily, until it was above the barrier entirely. Of course damping also reduces the tunneling rate, as shown by Caldeira and Leggett,[23] but a calculation of the tunneling rate in the absence of damping provides a useful starting point, giving an upper bound on the resistance R_0. We also ignore any effect of phase coherent reflections from subsequent wells of the Josephson potential. This is expected to be a significant source of error, especially for values of $x > 1$, in which case $\psi(\phi)$ is expected to be significantly spread out over more than one potential well.

We assume that Γ^+, the tunneling rate to the right (downhill) and Γ^-, the tunneling rate to the left are independent. We obtain, as in the classical case,

$$R_0 = \frac{\hbar}{2e}\frac{1}{I}\frac{d\phi}{dt} \approx \frac{\hbar}{2e}\frac{1}{I}2\pi(\Gamma^+ - \Gamma^-)\,. \tag{17}$$

To obtain a first estimate of R_0 we use the Wentzel-Kramers-Brillouin (WKB) approximation result for Γ. The tunneling rate has been estimated by other authors to be[23–26]

$$\Gamma=\frac{\omega_0}{2\pi}\chi\sqrt{v}\,\exp(-vs)\ , \tag{18}$$

where $v=(V_b/\hbar\omega_0)^{1/2}$, V_b is the barrier height, equal to $2E_J-hI/4e$, ω_0 is the classical resonant frequency of the well, $\hbar\omega_0=(8E_JE_c)^{1/2}$, at $I\ll I_{c0}$, χ and s are numerical constants, which are functions of the shape of the potential and of the damping. For the cubic potential approximation, and assuming low damping $\chi\approx 52.1$, $s\approx 7.2$.[23–26] Combining (17) and (18), we obtain an analytical estimate for R_0, which we compare with the measured low-temperature values in Fig. 19. While the value of R_0 for the sample with $R_n=14.8$ kΩ ($x\approx 0.25$) is in agreement with the estimate, the samples with large x exhibit values of R_0 considerably lower than the estimate.

One large source of discrepancy in the above comparison is the inaccuracy of WKB tunneling estimates for values of $x>1$. In this range, the width of $\psi(\phi)$ becomes comparable to the well spacing, and only one energy level is found in the well. Thus the semiclassical WKB approximation is no longer appropriate. To obtain a better estimate for the tunneling rate in the regime with x near 1, we have carried out a numerical calculation. We isolate a single well of the Josephson potential by considering the potential U_A shown in Fig. 20. For any energy, one can integrate the Schrödinger equation to find the resulting wave function $\psi_E(\phi)$. We consider an initial condition $\psi(\phi,t=0)=\psi_0(\phi)$ chosen to be essentially localized in the potential well; $\psi_0(\phi)$ is defined by us as the ground state of the potential U_B shown in Fig. 20. We then expand $\psi_0(\phi)$ using the $\psi_E(\phi)$ wave functions, and compute the time evolution $\psi(\phi,t)$. Finally, we can extract the probability that the system has *not* tunneled, which we call $P(t)$, from the projection of $\psi(\phi,t)$ on $\psi_0(\phi)$; $P(t)\propto|\int\psi_0(\phi)^*\psi(\phi,t)d\phi|^2$. We define a normalized spectral weight

$$f(E)=\frac{\left|\int\psi_0^*(\phi)\psi_E(\phi)d\phi\right|^2}{A}\ , \tag{19}$$

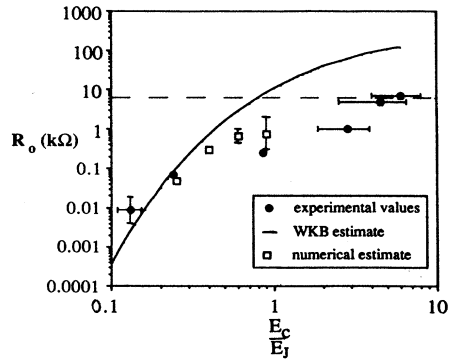

FIG. 19. R_0 vs $x=E_c/E_J$. Comparison of experimental values, values obtained using the WKB approximation, and values obtained numerically. The dashed horizontal value indicates the value of the quantum resistance $R_Q=h/4e^2$.

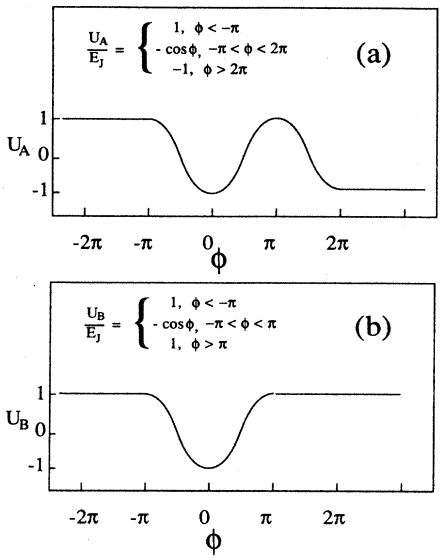

FIG. 20. The two different potentials used in the numerical calculations of R_0. (a) Metastable potential, used to calculate ψ_E. (b) Stable potential, used to calculate ψ_0.

where A is the normalization constant given by $A=\int\psi_0(\phi)^*\psi_0(\phi)d\phi\int\psi_E(\phi)^*\psi_E(\phi)d\phi$. We then have

$$P(t)=\left|\int dE\,f(E)e^{-iEt/\hbar}\right|^2\ . \tag{20}$$

Insofar as the shape of $f(E)$ is approximately Lorentzian, with full width at half maximum of δE, then we may approximate $P(t)$ by a function of the form $e^{-t/\tau}$. The escape rate τ^{-1} is then given by

$$\frac{\hbar}{\tau}=\delta E\ . \tag{21}$$

Figure 21 shows a comparison of escape rates calculat-

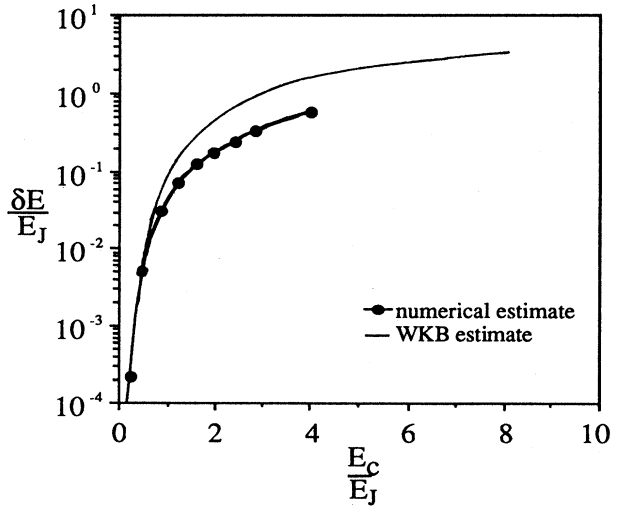

FIG. 21. Comparison of WKB and numerical estimates for the escape rate, expressed as a normalized energy width, and therefore only dependent on x. $\delta E=\hbar/\tau$, where $1/\tau$ is the escape rate.

ed with the WKB formula (18) and by the numerical technique discussed above. We see that, while for values of $x \ll 1$ the results of the two calculation methods converge, for $x > 0.5$ there is considerable discrepancy, as expected; the tunneling rate calculated by the wave-function expansion method outlined above is significantly lower. In particular, note that the numerical estimate yields $\delta E < E_J$, which is self-consistent, whereas the WKB escape rates give $\delta E > E_J$, which is conceptually inconsistent with the escape out of a well of depth E_J. This systematic difference in lifetime is also in the right direction to improve the agreement with the observed values of R_0.

We obtain direct numerical estimates for R_0 by calculating the escape rates Γ^+ and Γ^- after small positive and negative (respectively) currents have been applied, tilting the potential. The numerical estimates for R_0 are shown in Fig. 19, in comparison with the WKB estimates and the experimental values. While the wave-function expansion method allows us to obtain reasonable estimates in the regime with x near 1, where WKB methods have broken down, its range of validity is also limited. As x becomes larger than one, the range of bias current I giving a constant R_0 is very small, making estimates of R_0 very inaccurate. For x distinctly larger than 1, the calculated $f(E)$ also no longer resembles a Lorentzian bell shape, and $P(t)$ can no longer be approximated by a decaying exponential. At this point the quantum phase uncertainty approaches one well spacing, and our assumption of a well-defined exponential escape rate necessary for evaluating (17) breaks down: Other methods must be used to estimate R_0. The numerical calculations are an improvement over the WKB estimates, but a more refined model, perhaps taking into account coherent reflections between subsequent wells, is needed.

While our model is inaccurate for $x > 1$, it provides a very good account of the behavior of our sample with normal resistance 14.8 kΩ. For this sample, x is only about 0.25, so that $\psi(\phi)$ should have relatively small width compared to the spacing between Josephson potential wells, and our model appears reasonable. As shown in Fig. 22, the estimated value is in very good agreement with the low-temperature value of R_0. Moreover, the crossover temperature at which the system apparently goes from this quantum tunneling limit to thermally activated escape is in excellent agreement with the $\hbar\omega_p/2\pi k_B$, as expected from (7). The predicted values of $R_0(0)$ and of $T_{\text{crossover}}$ contain no adjustable parameters: R_n is measured, and the capacitance is given by the estimated intrinsic capacitance C_i. This value of the capacitance is also in agreement with that involving the charging effects described in Sec. II B 2, and interpreted below in Sec. III D 3.

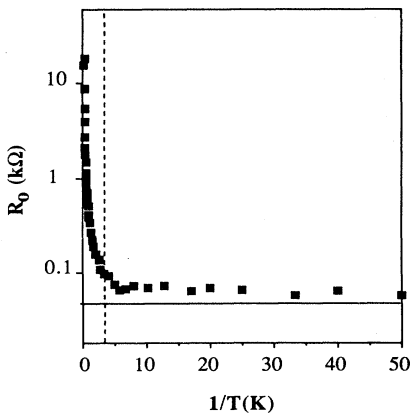

FIG. 22. R_0 vs T^{-1} for the sample with $R_n = 14.8$ kΩ. The horizontal line is the zero-temperature estimate obtained by numerical methods. The dashed vertical line corresponds to $T = \hbar\omega_p/2\pi k_B$, at which the crossover to the quantum limit should occur.

From Fig. 19, it is apparent that characteristic low-T values of R_0 approach a value of order $R_Q = h/4e^2 \approx 6.1$ kΩ. We do not believe this to be fortuitous. If we take a maximum reasonable energy level width equal to the barrier height $\delta E \approx 2E_J \pm hI/4e$, the net escape rate to the right becomes $\Gamma^+ - \Gamma^- = (2\pi)I/2e$. Using (17), we have $R_0 = (h/2eI)(2\pi)(I/2e) = (2\pi)h/4e^2$.

3. *Interpretation of the critical current I_c*

Having developed a picture of the evolution of the system which gives rise to a linear resistive voltage at low current values, we now address the question of the critical current, i.e., up to what current level is this regime of slow phase slippage locally stable? As we have seen in the semiclassical regime, two aspects must be considered. There is an absolute limit (I_{c0} in the semiclassical case) set by the binding energy of the phase-locked state, and there is a dynamic limit (I_r in the semiclassical case) set by the dissipation which prevents runaway and causes continual retrapping into the slow phase-slip (low voltage) regime. In the quantum regime, we are only able to provide an estimate for the "binding energy" of the phase-locked state. Our estimate should thus serve as an approximate upper bound for the actual critical current I_c. *Quantitative* estimates for a "dynamic" critical current, which take into account the device's relaxation by dissipation, are difficult in the quantum regime, and will be left to future work.

Because the state of the system is time-dependent in the presence of a current, which causes phase slippage, there is no simple way to find the analogue of the classical maximum supercurrent I_{c0}, even at $T = 0$. However it seems plausible to argue that, just as $I_{c0} = 2eE_J/\hbar$ in that case, where E_J is the binding energy due to the cosine potential, in this case we might expect $I_c = (2e/\hbar)E_B$ where E_B is the binding energy given by (16). The rationale is this: The work done by the current in an incremental phase shift is $(\hbar/2e)I\,d\phi$. For stability, this must be less than $dE = [dE(\phi)/d\phi]d\phi$. This leads to $I < (2e/\hbar)[dE(\phi)/d\phi]_{\max}$, or $2eE_J/h$ for the classical case $E(\phi) = -E_J\cos\phi$. If we assume that E_B is lost for a phase shift $\Delta\phi \approx 1$ in the quantum case as well, it follows that $I_c \approx (2e/\hbar)E_B$. In particular, in the limit where $E_J \ll E_c$, we have $E_B = E_J^2/8E_c$, which leads to

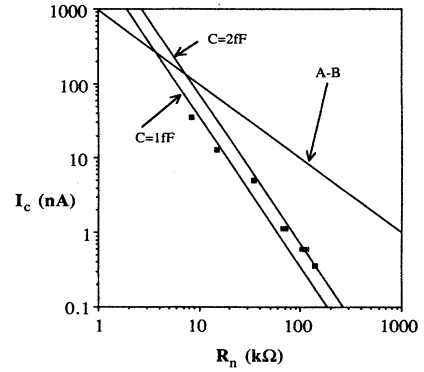

FIG. 23. Measured critical current I_c (at $H=0$ and $T=30$ mK) for six samples (black squares). The A-B line is the Ambegaokar-Baratoff critical current prediction. The other two lines are our estimate (24a), plotted for two reasonable capacitance values.

$$I_c=(E_J/8E_c)I_{c0}\ . \tag{22}$$

Insofar as this formula is correct, the observed I_c should scale with R_n^{-2} rather than with R_n^{-1} as does I_{c0}. In fact, just such a scaling of R_n^{-2} of I_c (extrapolated to $T=0$) is found for our highest-resistance samples as shown in Fig. 23. Moreover, the absolute numerical magnitudes are also in reasonable agreement if E_c is based on the same capacitance values of 1–2 fF used earlier in interpreting R_0. Again, this must be considered quite satisfactory in view of the approximate nature of the argument.

In a recent Comment on Ref. 3, Mirhashem and Ferrell[48] (MF) have suggested a similar estimate for the reduction in I_c due to quantum phase fluctuations. They estimate the linear response of a Josephson junction by

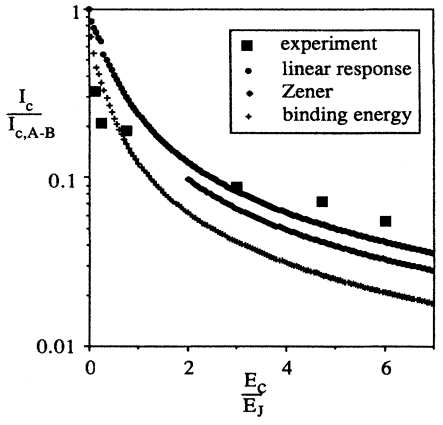

FIG. 24. Measured critical current I_c (at $H=0$ and $T=30$ mK) for six samples (black squares), plotted against the estimated ratio of charging to Josephson coupling energy. Two of the estimates shown are obtained by our binding energy method and by the linear response method by Mirhashem and Ferrell (Ref. 48), described in Sec. III C. The third estimate is our Zener tunneling estimate (only valid at large E_c/E_J), described in Sec. III D.

calculating the inverse inductance of the device $L^{-1}=(2e/\hbar)^2E_J\langle\cos\phi\rangle$, where $\langle\ \rangle$ denotes the ground-state expectation value. As the ratio of E_c to E_J increases, quantum fluctuations increase, and $\langle\cos\phi\rangle$ decreases. Assuming that the critical current scales with the linear response (as it does in the absence of fluctuations) they obtain, at large $x=E_c/E_J$,

$$I_c=(E_J/4E_c)I_{c0}\ , \tag{23}$$

which is a factor of 2 larger than (22). Figure 24 shows a comparison of these two I_c estimates calculated for $0<x<7$, a range covering all our experimental data. While the MF estimate is closer to the experimental values for large x, both approaches provide reasonably satisfactory agreement, given their approximate nature and the experimental uncertainty in C.

D. The quantum limit: Q-space description

The simple analysis we have provided in the above sections is successful in providing a semiquantitative account of our observations in the regime with Josephson energy of order the charging energy ($x\approx 1$). As we decrease the Josephson energy further, quantum phase fluctuations increase, and the behavior of the devices becomes increasingly difficult to characterize by models based in ϕ space. It is useful to consider the opposite viewpoint.

1. The energy band spectrum

Several authors[11,49–57] have investigated Josephson junction dynamics in charge space, looking at the behavior of Q, the quantum-mechanical conjugate of ϕ. The energy spectrum of the Josephson device then assumes a bandlike structure, reminiscent of that of a one-dimensional crystal. Such models appear particularly appropriate for the case $E_c\gg E_J$ (that is, $x\gg 1$), where the band structure approaches that of a free particle, with small energy gaps caused by the periodic Josephson potential. Figure 25 represents a theoretical energy spectrum for parameters in this regime, derived by Guinea and Schön.[55] The variable on the horizontal axis is Q_x, the charge applied to the device by external means (such as a current source). The qualitative behavior of the device is simple: The device can charge up, as a common capacitor, but it can only discharge by having electrons tunnel from one electrode to the other. While the charging-up process is continuous, the discharge by tunneling is discrete, in units of e (single electrons) or $2e$ (Cooper pairs). In this limit, E_J is the width of the gaps at $Q_x=\pm e$, where the "kinetic energy" $Q^2/2C=e^2/2C=E_c$. (In the opposite limit $x\ll 1$, because of the negligible MQT between adjacent minima, the bands approach zero width, and low-lying ones are separated by the plasma energy.)

In the presence of an imposed current I feeding charge onto the electrodes, the external charge variable Q_x advances at a rate $dQ_x/dt=I$. The instantaneous voltage is given by $V=dE/dQ_x$. While the energy spectrum may appear straightforward, the motion of the system along

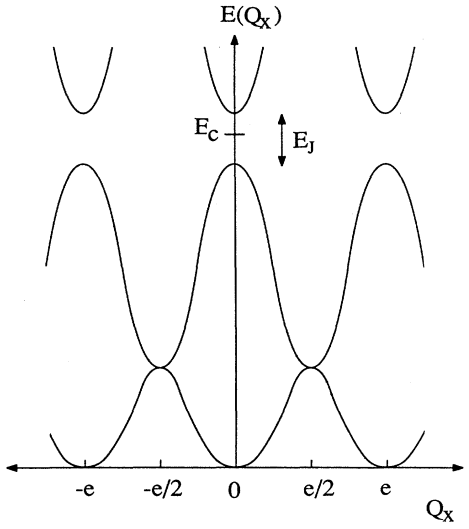

FIG. 25. Sketch of the energy spectrum as a function of applied charge Q_x derived for a Josephson junction in the limit $E_c \gg E_J$. The figure is adapted from Ref. 55.

the energy band may be quite complex, even if we assume a perfect current source (an assumption which we later relax). If we begin at $Q_x=0$, the system can at first only charge up capacitively. Once Q_x is greater than $e/2$, however, the system can either proceed upward, continuing to accumulate charge on one electrode, or it can relax to the lower band, by having a single electron tunnel from one electrode to the other. Moreover, if the current is large enough, the system can Zener tunnel to the higher bands, as described below (which corresponds to charging up faster than electrons can tunnel to equalize the built-up charge). Depending on the values of these various relaxation times, the size of the band gaps, and the actual nature of the current source, one can obtain very different dynamics, corresponding to a large variety of possible I-V curves.

This analytic framework can be used to provide an alternative version of the arguments given above in interpreting the observed depressed values of I_c. Moreover, this framework can also be used to explore the regime in which $E_c \gg E_J$, to provide a theoretical background for an interpretation of I-V curves exhibiting apparent knees at $V=e/2C$, of the type shown in Fig. 3.

2. *Determination of I_c*

As the current $I=dQ/dt$ increases, there is an increasing probability that the system will jump from the maximum of the lower band at the zone boundary into the next higher band rather than continuing to cycle up and down in the lowest band. By simply transcribing the usual calculation of this Zener tunneling probability to the present context, we have previously shown[1] that the probability of a jump on each cycle is

$$P_{\text{Zener}}=\exp\left[-\frac{\pi^2 E_J^2}{8E_c(\hbar I/2e)}\right]=\exp\left[-\frac{I_Z}{I}\right], \tag{24}$$

where

$$I_Z=\pi e E_J^2/8\hbar E_c\ . \tag{24a}$$

Here I_Z is just $\pi/2$ times larger than the I_c found in (22), or $\pi/4$ times the estimate in (23), both obtained starting from the ϕ-space framework, described in Sec. III C. In particular, all three results share the property that I_c scales with E_J^2 or R_n^{-2}, rather than with the first powers of these quantities, as does I_{c0}. The physical picture we have is that, for $I<I_Z$, occasional Zener tunneling occurs, but the system quickly relaxes back down to the lowest band. The associated dissipation contributes to the resistance R_0, but this does not spell the end of the low-voltage regime. Rather, we associate the end of this regime with the complete breakdown of the band gap, allowing the system to run up onto the upper, free-particle-like bands, where it acts "normal," i.e., as if E_J were zero. It is, of course, arbitrary to associate this I_Z, where P_{Zener} is just $1/e$, with the observed I_c, but because of the exponential dependence, one might expect this criterion to be correct to within a factor of 2; hence the three estimates (22), (23), and (24) are consistent within their expected accuracy.

At $T>0$, the probability of thermal excitation across the band gap E_J would be expected to be approximately given by e^{-E_J/k_BT} on each cycle of the Bloch oscillation. If this probability is added to that given by (24), and the sum set equal to $1/e$ in analogy to the above argument, we obtain a simple phenomenological estimate for the effect of temperature in reducing I_c. This argument gives the correct characteristic temperature for substantial reduction in I_c, namely E_J/k. This rough estimate is plotted in Fig. 5(b).

In this approach, as in the ϕ-space one, damping during the MQT process is expected to have a strong effect in reducing the tunnel probability, and hence increasing the estimated critical current. The physical arguments of Buettiker and Landauer[58] suggest that we can still use

$$\frac{dE}{d\phi}=-\frac{\hbar}{2eR}\left[\frac{2(E+E_J\cos\phi)}{C}\right]^{1/2} \tag{25}$$

(which was discussed in Sec. III B in the semiclassical regime) at least approximately in the MQT case by taking the absolute value of the quantity inside the brackets. Thus in the present case it has a similar value in the barrier and in the well. However, the question is what value of R is physically correct to be inserted into this formula. We can say that $R\approx R_n$ would be consistent with our data, in that it would introduce rather modest corrections which could be accommodated by choosing a different criterion for I_c, such as the criterion that P_Z be set equal to e^{-2} rather than e^{-1}. On the other hand, R_L is so large that its damping effects would be negligible in this regime. Likewise, R_0 is sufficiently below R_n at low temperatures that it would, if applicable, give such large corrections as to be very difficult to reconcile with the data. Even more inconsistent with the data would be any damping resistance comparable with the impedance of free space $Z_0=377\ \Omega$, such as the characteristic impedance of the leads attached to the junction.

3. *Coexistence of Coulomb blockade and Josephson tunneling*

In the previous sections, we have provided a number of semiquantitative models accounting for the basic features of our observed zero-magnetic-field I-V curves. As described above, however, we also performed a second set of experiments: By applying a magnetic field to the junctions, we depressed the Josephson coupling even further. At low field values we obtained measurements similar to the ones made at zero field, with increasing R_0 and decreasing I_c, as the field was increased. In all three samples measured as a function of magnetic field, however, a new regime was discovered, exemplified by the I-V curve shown in Fig. 3. As mentioned above, the striking feature of this regime is the *coexistence* of a sharp knee at a voltage corresponding to $e/2C$, with a very sharp voltage jump at a "critical current" I_c.

We have proposed[3] the following simplified phenomenological picture: The difference in electrostatic energy due to the transfer of a single electron is $e^2/2C$. In our samples this energy is large, typically of order 1 K. At low voltages, below $e/2C$, the system does not acquire enough energy from the source in the tunneling process to offset the difference in electrostatic energy involved. Tunneling is therefore energetically unfavorable and is inhibited, provided the temperature is low enough for thermal-activation processes to freeze out. This yields a static situation; electrons are "trapped" on the junction electrodes and the dynamic resistance is extremely high. As V becomes greater than $e/2C$, on the other hand, a single electron transfer becomes energetically favorable, and the differential resistance decreases, giving rise to a knee in the I-V curve at that voltage. In this dynamic regime, if the instantaneous voltage increases beyond e/C, it becomes energetically favorable also for Cooper pairs to tunnel, and the voltage is driven back down. The observed average voltage is thus restricted to a value below e/C, until the system's ability to transfer Cooper pairs is exceeded at $I=I_c$. It thus appears that Josephson tunneling plays an important role in the explanation of the observed plateau in the I-V curve and the subsequent critical current.

This explanation can be restated in terms of the band model described in Sec. III D 1. The highly resistive part of the I-V curve may then be due to the system being trapped at a fixed charge on the lowest band. This configuration is, however, only stable for $V<e/2C$. At higher (average) voltages, the system must spend time in higher bands and tends to relax to lower bands by electron tunneling, conducting charge, and reducing the differential resistance of the device. This happens until the current is large enough for Zener processes to become so likely that the Josephson band gaps are ineffective at keeping the system in low bands. At this point ($I=I_c$) the voltage rises sharply to the energy gap.

IV. CONCLUSIONS

We have experimentally investigated the competition between charging, Josephson, and thermal energies in small tunnel junctions. Furthermore, we have presented a series of simple phenomenological models which provide satisfactory semiquantitative explanations of some of the startling phenomena observed experimentally, and may be a useful starting point for more rigorous theoretical treatments. Our most important findings are outlined below.

If the Josephson energy is much larger than the charging energy, we find the usual current-voltage characteristics found in conventional low-resistance Josephson junctions. However, we find that as the charging energy becomes important, the behavior of the devices changes completely.

When the charging and Josephson energy are of comparable magnitude, the I-V characteristic is always resistive, even at low currents $I<I_c$; apparently the very low Josephson barrier height, comparable to k_BT or to the energy-level width, causes very frequent phase slips, due to thermal activation and/or quantum tunneling. The critical current itself, now defined as the current at which the average phase-slip rate sharply increases to the energy gap frequency, is greatly reduced below the unfluctuated Ambegaokar-Baratoff critical current I_{c0}, even at the lowest temperatures, and apparently scales with the binding energy of the ground state, i.e., with R_n^{-2} for $E_c \gg E_J$.

If the Josephson energy becomes much smaller than the charging energy, the I-V characteristic becomes very resistive ($R \approx R_L \gg R_n$) at low currents, with a sharp knee at a voltage apparently corresponding to $e/2C$. The average phase-slip rate increases very quickly at low currents, as the Josephson potential seems too weak to localize ϕ. While quantum fluctuations in ϕ are presumably large, the charge now seems classically well defined, as indicated by the knee at $e/2C$, the voltage difference required before the tunneling of a single electron becomes favored by the capacitive energy $Q^2/2C$.

ACKNOWLEDGMENTS

The authors are indebted to H. Rogalla for his generous assistance in setting up the electron-beam writing facility used in patterning the samples. The authors also acknowledge discussions with E. Ben-Jacob, M. J. Burns, S. Chakravarty, J. Clarke, A. Cleland, A. T. Dorsey, M. P. A. Fisher, T. Fulton, Y. Gefen, B. I. Halperin, R. L. Kautz, K. Mullen, and G. Schön. This research was supported in part by National Science Foundation Grant No. DMR-84-04489, Office of Naval Research Contract No. N00014-83-K-0383, and by Joint Services Electronics Program Contract No. N00014-84-K-0465.

[1]M. Iansiti, A. T. Johnson, W. F. Smith, H. Rogalla, C. J. Lobb, and M. Tinkham, Phys. Rev. Lett. **59**, 489 (1987).

[2]M. Iansiti, A. T. Johnson, W. F. Smith, C. J. Lobb, and M. Tinkham, Jpn. J. Appl. Phys. Suppl. **26-3**, 1557 (1987).

[3]M. Iansiti, A. T. Johnson, C. J. Lobb, and and M. Tinkham, Phys. Rev. Lett. **60**, 2414 (1988).

[4]T. A. Fulton and G. J. Dolan, Phys. Rev. Lett. **59**, 109 (1987).

[5]I. Giaever and H. R. Zeller, Phys. Rev. Lett. **20**, 1505 (1968).

[6]J. Lambe and R. C. Jaklevic, Phys. Rev. Lett. **22**, 1371 (1969).
[7]R. E. Cavicchi and R. H. Silsbee, Phys. Rev. Lett. **52**, 1453 (1985); R. E. Cavicchi and R. H. Silsbee, Phys. Rev. B **37**, 706 (1988).
[8]J. B. Barner and S. T. Ruggiero, Phys. Rev. Lett. **59**, 807 (1987).
[9]P. J. M. van Bentum, H. van Kempen, L. E. C. van de Leemput, and P. A. A. Teunissen, Phys. Rev. Lett. **60**, 369 (1988).
[10]U. Hartmann, R. Berthe, and C. Heiden (unpublished).
[11]D. V. Averin and K. K. Likharev, J. Low Temp. Phys. **62**, 345 (1986).
[12]H. Akoh, O. Liengme, M. Iansiti, M. Tinkham, and J. U. Free, Phys. Rev. B **33**, 2038 (1986).
[13]G. J. Dolan, Appl. Phys. Lett. **31**, 337 (1977); G. J. Dolan, R. E. Miller, R. A. Linke, T. G. Phillips, and D. P. Woody, IEEE Trans. Magn. **MAG-17**, 684 (1981).
[14]E. L. Hu, L. D. Jackel, and R. E. Howard, IEEE Trans. Electron. Dev. **ED-28**, 1382 (1981).
[15]W. C. Danchi, Ph.D. thesis, Harvard University, Cambridge, MA, 1982.
[16]T. C. Wang and R. I. Gailey, Phys. Rev. B **18**, 293 (1978).
[17]R. H. Ono, M. J. Cromar, R. L. Kautz, R. L. Soulen, J. H. Colwell, and W. E. Fogle, IEEE Trans. Magn. **MAG-23**, 1670 (1987).
[18]V. Ambegaokar and A. Baratoff, Phys. Rev. Lett. **10**, 486 (1963).
[19]W. C. Stewart, Appl. Phys. Lett. **12**, 277 (1968).
[20]D. E. McCumber, J. Appl. Phys. **39**, 3113 (1968).
[21]J. M. Martinis, M. H. Devoret, and J. Clarke, Phys. Rev. Lett. **55**, 1543 (1985); M. H. Devoret, J. M. Martinis, and J. Clarke, *ibid.* **55**, 1908 (1985).
[22]G. E. Blonder, M. Tinkham, and T. M. Klapwijk, Phys. Rev. B **25**, 4515 (1982).
[23]A. O. Caldeira and A. J. Leggett, Phys. Rev. Lett. **46**, 211 (1981); A. O. Caldeira and A. J. Leggett, Ann. Phys. (N.Y.) **149**, 374 (1983).
[24]L. D. Chang and S. Chakravarty, Phys. Rev. B **29**, 130 (1984); **30**, 1566(E) (1984).
[25]H. Grabert, in *IC SQUID Berlin, 1985,* edited by H. D. Hahlbohm and H. Lubbig (deGruyter, Berlin, 1985), and references therein.
[26]P. Hänggi, Ann. N.Y. Acad. Sci. **480**, 51 (1986), and references therein.
[27]V. Ambegaokar, U. Eckern, and G. Schön, Phys. Rev. Lett. **48**, 1745 (1982); U. Eckern, G. Schön, and V. Ambegaokar, Phys. Rev. B **30**, 6419 (1984).
[28]T. Fulton and L. N. Dunkleberger, Phys. Rev. B **9**, 4760 (1974).
[29]M. Naor, C. D. Tesche, and M. B. Ketchen, Appl. Phys. Lett. **41**, 202 (1982).
[30]M. H. Devoret, J. M. Martinis, D. Esteve, and J. Clarke, Phys. Rev. Lett. **53**, 1260 (1984).
[31]W. C. Danchi, J. B. Hansen, M. Octavio, F. Habbal, and M. Tinkham, Phys. Rev. B **30**, 2503 (1984).
[32]P. Silvestrini, S. Pagano, R. Cristiano, O. Liengme, and K. E. Gray, Phys. Rev. Lett. **60**, 844 (1988); P. Silvestrini, O. Liengme, and K. E. Gray, Phys. Rev. B **37**, 1525 (1988).
[33]H. A. Kramers, Physica (Utrecht) **7**, 284 (1940).
[34]V. Ambegaokar and B. I. Halperin, Phys. Rev. Lett. **22**, 1364 (1969).
[35]P. A. Lee, J. Appl. Phys. **42**, 325 (1971).
[36]J. Kurkijärvi, Phys. Rev. B **6**, 832 (1972).
[37]M. Büttiker, E. P. Harris, and R. Landauer, Phys. Rev. B **28**, 1268 (1983).
[38]A. Barone, R. Cristiano, and P. Silvestrini, J. Appl. Phys. **58**, 3822 (1985).
[39]W. den Boer and R. de Bruyn Ouboter, Physica **98B**, 185 (1980).
[40]R. J. Prance, A. P. Long, T. D. Clark, A. Widom, J.E. Mutton, J. Sacco, M. W. Potts, G. Megaloudis, and F. Goodall, Nature (Paris) **289**, 543 (1981).
[41]R. F. Voss and R. A. Webb, Phys. Rev. Lett. **47**, 265 (1981).
[42]L. D. Jackel, J. P. Gordon, E. L. Hu, R. E. Howard, L. A. Fetter, D. M. Tennant, R. W. Epworth, and J. Kurkijärvi, Phys. Rev. Lett. **47**, 697 (1981).
[43]S. Washburn, R. A. Webb, R. F. Voss, and S. M. Faris, Phys. Rev. Lett. **54**, 2712 (1985).
[44]D. B. Schwartz, B. Sen, C. N. Archie, and J. E. Lukens, Phys. Rev. Lett. **55**, 1547 (1985).
[45]H. Grabert and U. Weiss, Phys. Rev. Lett. **53**, 1787 (1984).
[46]R. Cristiano and P. Silvestrini, IEEE Trans. Magn. **MAG-23**, 771 (1987); R. Cristiano and P. Silvestrini, J. Appl. Phys. **60**, 3243 (1986).
[47]E. Ben Jacob, D. J. Bergman, B. J. Matkowsky, and Z. Schuss, Phys. Rev. A **26**, 2805 (1982).
[48]B. Mirhashem and R. A. Ferrell, Phys. Rev. Lett. **61**, 483 (1989).
[49]S. Chakravatry, Phys. Rev. Lett. **49**, 681 (1982).
[50]A. Schmid, Phys. Rev. Lett. **51**, 1505 (1985).
[51]K. K. Likharev and A. B. Zorin, J. Low Temp. Phys. **59**, 347 (1985).
[52]K. Mullen, E. Ben-Jacob, and Z. Schuss, Phys. Rev. Lett. **60**, 1097 (1988); E. Ben-Jacob, Y. Gefen, K. Mullen, and Z. Schuss, Phys. Rev. B **37**, 7400 (1988); in Ref. 25.
[53]A. Widom, G. Megaloudis, T. D. Clark, H. Prance, and R. J. Prance, J. Low Temp. Phys. **57**, 651 (1984), and references therein.
[54]M. P. A. Fisher and W. Zwerger, Phys. Rev. B **32**, 6190 (1985); W. Zwerger, *ibid.* **35**, 4737 (1987); M. P. A. Fisher, Phys. Rev. Lett. **57**, 885 (1986).
[55]F. Guinea and G Schön, Europhys. Lett. **1**, 585 (1986); J. Low Temp. Phys. **69**, 219 (1987).
[56]M. Büttiker, Phys. Rev. B **36**, 3548 (1987).
[57]R. J. Prance, T. D. Clark, J. E. Mutton, H. Prance, T. P. Spiller, and R. Nest, Phys. Lett. **107A**, 133 (1985); H. Prance, R. J. Prance, T. P. Spiller, J. E. Mutton, T. D. Clark, and R. Nest, *ibid.* **111A**, 199 (1985).
[58]M. Büttiker and R. Landauer, IBM J. Res. Dev. **30**, 451 (1986).

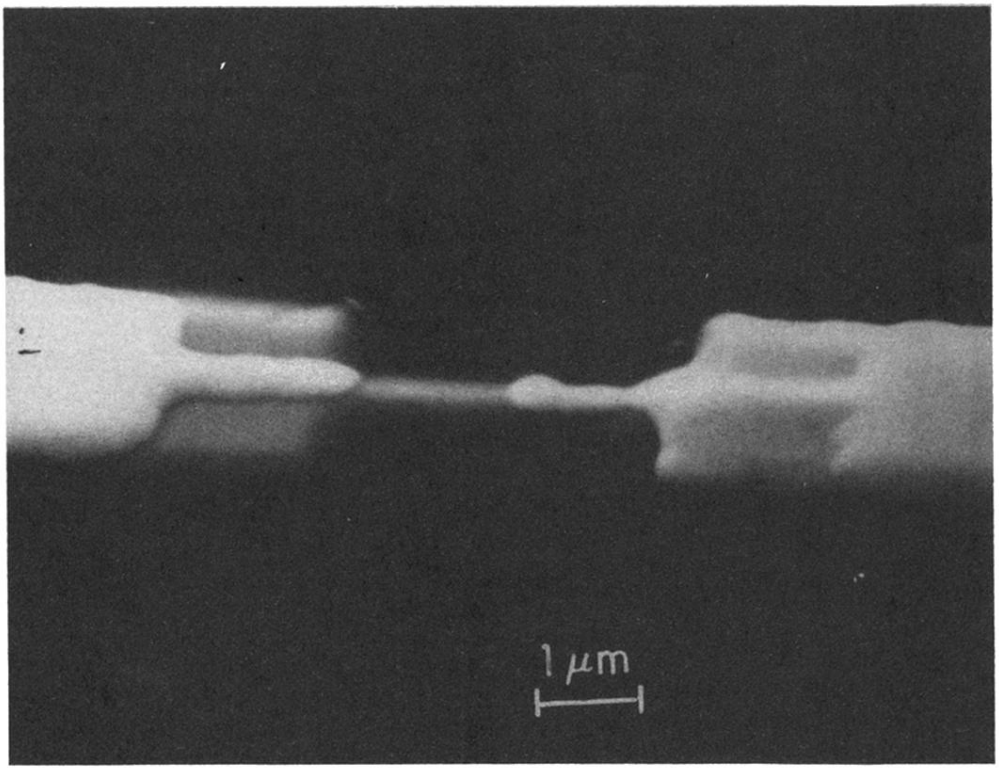

FIG. 4. Scanning electron microscope photograph of a previously measured sample with area 0.1 $(\mu m)^2$, normal resistance $R_n = 35$ kΩ, and capacitance $C \approx 2$ fF.